ALDOT

Alabama Department of Transportation

National Center for Asphalt Technology

NCAT

at AUBURN UNIVERSITY

ALDOT Research Project 931-106S

Technical Assistance for Quantifying Emissions from Asphalt Mixtures

Final Report

March 2025

1. Report No.	2. Government Accession No.	3. Recipient's Catalog No.	
4. Title and Subtitle Technical Assistance for Quantifying Emissions from Asphalt Mixtures		**5. Report Date** March 2025 **6. Performing Organization Code**	
7. Author(s) M. Sadeghi, B. K. Bairgi, Z. Hartzog, S. Gatiganti, N. Tran, H. Dylla, B. Bowers		**8. Performing Organization Report No.**	
9. Performing Organization Name and Address National Center for Asphalt Technology at Auburn University 277 Technology Parkway Auburn, AL 36830		**10. Work Unit No.** **11. Contract or Grant No.** ALDOT Research Project 931-106S	
12. Sponsoring Agency Name and Address Alabama Department of Transportation Bureau of Research and Development 1409 Coliseum Boulevard Montgomery, AL 36110		**13. Type of Report and Period Covered** Final Report April 2023 – March 2025 **14. Sponsoring Agency Code**	
15. Supplementary Notes			

16. Abstract

This study evaluated the effects of using Warm Mix Asphalt (WMA) technologies to reduce asphalt production temperatures on energy consumption and pavement performance in Alabama. Two field experiments were conducted. The first compared two chemical WMA mixtures to a conventional Hot Mix Asphalt (HMA), while the second used one of the WMA technologies from the first experiment to explore further temperature reductions.

Each experiment included field construction, burner fuel monitoring, and laboratory performance testing using IDEAL-CT, HWTT, HT-IDT, and AMPT tests. Long-term fatigue and rutting performance were predicted using FlexPAVE™ modeling.

Reducing production temperatures by 40°F and 65°F resulted in burner fuel savings of approximately 8% and 19%, respectively. WMA mixtures demonstrated comparable or improved cracking resistance but generally showed reduced rutting resistance, particularly at the lowest production temperature evaluated. Additionally, FlexPAVE™ modeling predicted slightly higher fatigue damage and rutting for WMA mixtures compared to HMA.

Overall, the results support the use of WMA technologies to reduce energy consumption while maintaining acceptable performance. However, when WMA is produced at significantly lower temperatures, mix design adjustments may be needed to ensure rutting resistance meeting specification requirements.

17. Key Words		18. Distribution Statement	
Warm Mix Asphalt, Energy Consumption, Cracking, Rutting		No restrictions	
19. Security Classification (of this report) Unclassified	**20. Security Classification (of this page)** Unclassified	**21. No. of Pages** 58	**22. Price**

Acknowledgments

This project was sponsored by the Alabama Department of Transportation (ALDOT) and the Federal Highway Administration (FHWA). The project team at the National Center for Asphalt Technology (NCAT) would like to express their gratitude to all who contributed to this project. This includes individuals from ALDOT and FHWA, as well as the contractors and suppliers who made this work possible.

ALDOT Materials and Tests Bureau: Scott George, Chance Armstead, John Jennings, Steven Ingram, Tyler Hale.

ALDOT Research and Development Bureau: Kidada C. Dixon, Calvin Smith, Andre Jenkins, Michelle Gilmore.

ALDOT Office Engineer Bureau: Jimmy Carroll, Lynn Smith.

ALDOT Montgomery Area: Steve Wilson.

ALDOT Troy Area: Chris Huner.

FHWA: Mark Bartlet, Aaron Dawson, Kristy Harris, Latoya Johnson, Migdalia Carrion, Brittany Washington.

Alabama Asphalt Paving Association: Mel Monk.

APAC Alabama: Corey Wilson, Mike Fielding, Charles Cook, Scott Rich.

Wiregrass Construction Company: Brain Stuckey, Zach Pace.

Ingevity: Jenna Bowers.

Cargil: Dallas Little, Hassan Tabatabaee.

Ergon Aspahlt and Emulsion: Anthony Quattlebaum.

Table of Contents

List of Tables

List of Figures

1. INTRODUCTION

The asphalt paving industry continues to advance through the adoption of technologies that improve production efficiency, optimize material use, and enhance pavement longevity. Innovations such as warm mix asphalt (WMA), bio-based recycling agents, and balanced mix design (BMD) approaches have demonstrated significant potential to improve pavement performance and support more efficient use of available resources (Epps, 2019; Fakhri et al., 2021).

Among these innovations, WMA technologies have been widely studied for their ability to reduce production and placement temperatures, with benefits that include lower burner fuel consumption, improved mixture workability, and enhanced compaction. These advantages can extend paving seasons, improve consistency in meeting density requirements, and enable the use of higher percentages of reclaimed materials without compromising mixture performance (Jones, 2013; Prowell et al., 2012). While laboratory studies have consistently shown improvements in mixture performance and reductions in energy demand associated with WMA technologies, validation of these findings under field conditions remains limited (Hurley et al., 2009; West, Rodezno, Julian, Prowell, et al., 2014). As these technologies gain broader interest across the asphalt industry, transportation agencies and contractors recognize the importance of field-validated data to inform decisions regarding production practices and mixture design. Understanding how WMA technologies influence fuel consumption, mixture durability, and pavement performance in real-world conditions is essential for agencies and contractors seeking to balance operational efficiency with long-term pavement reliability.

Recognizing this need for field validation data, the Alabama Department of Transportation (ALDOT), in collaboration with the National Center for Asphalt Technology (NCAT), conducted this study to quantify burner fuel savings and assess mixture performance in field projects constructed with WMA technologies. This study was sponsored by the Federal Highway Administration (FHWA) to encourage state-led evaluations that link laboratory results with field application. Through this work, the research team aims to provide data-driven insights that will support informed decision-making for future specifications and mixture designs.

The following section outlines the specific objectives, the scope of the study, and the research approach used to quantify production efficiency and evaluate mixture performance when utilizing WMA technologies in field projects.

2. PROJECT OBJECTIVES AND SCOPE

The primary objective of this study was to evaluate the impact of reduced production temperatures, achieved through warm mix technologies, on burner fuel consumption and asphalt mixture performance characteristics. To support this objective, the study focused on the following specific goals:

- Quantify and compare burner fuel consumption during production through direct field measurements.
- Evaluate the effects of warm mix technologies on mixture cracking and rutting resistance using ALDOT's balanced mix design performance tests: the Indirect Tensile Asphalt

Cracking Test (IDEAL-CT) for cracking and the Hamburg Wheel-Tracking Test (HWTT) and High-Temperature Indirect Tensile Test (HT-IDT) for rutting.
- Assess the mechanical properties of the mixtures using Dynamic Modulus (E*), Cyclic Fatigue (CF), and Stress Sweep Rutting (SSR) tests.
- Estimate field performance of the evaluated mixtures using the FHWA's FlexMAT™ parameters and FlexPave™ v2.2 mechanistic models.

The study included two field experiments constructed according to ALDOT specifications, as follows:

- **Experiment 1** included a control hot mix asphalt (HMA) section and two sections produced with chemical WMA technologies to establish baseline performance and production efficiency comparisons.
- **Experiment 2**, developed based on findings from Experiment 1, focused on evaluating further reductions in production temperatures and their impacts on both burner fuel consumption and mixture performance.

The NCAT research team, along with the contractor for each project, monitored all phases of mixture production and field construction, collected real-time data on burner fuel consumption, and sampled loose mixtures directly from the asphalt plant. These samples were then transported to the NCAT laboratory for performance testing to support the evaluation of the constructed field sections.

3. LITERATURE REVIEW

3.1 Warm Mix Asphalt (WMA): Definition, Mechanisms, and Technologies

The production of conventional HMA typically involves heating aggregates and asphalt binder to temperatures between 300°F and 350°F. These elevated temperatures are necessary to ensure proper aggregate drying, effective binder coating, and adequate mixture workability and compaction. However, this process requires considerable fuel consumption and results in emissions associated with high-temperature operations (Milad et al., 2022). In response to ongoing industry efforts to enhance production efficiency and operational flexibility, WMA technologies have been developed. These technologies allow asphalt mixtures to be produced and placed at temperatures typically ranging from 230°F to 275°F, representing reductions of 30°F to 70°F compared to conventional HMA (Gandhi et al., 2009; Prowell et al., 2012).

The ability to reduce production temperatures without compromising mixture workability or compaction is achieved by decreasing binder viscosity or improving binder-aggregate interaction, which improves mixture workability and facilitates compaction, even under challenging conditions such as cooler climates or extended haul distances. This capability helps contractors meet density specifications more reliably and allows agencies to extend paving windows and increase project flexibility (Capitão et al., 2012; Rubio et al., 2012; Sukhija et al., 2022).

WMA technologies are generally categorized based on the mechanism used to lower production temperatures:

- **Foaming technologies** introduce controlled amounts of water into hot asphalt under pressure, causing the binder to foam and temporarily expand. This expansion reduces binder viscosity and improves coating efficiency and workability (Cheraghian et al., 2020).
- **Organic (wax-based) additives** include waxes and fatty amides that lower binder viscosity at elevated temperatures, improving coating and compaction. These additives also crystallize at lower temperatures, contributing to rutting resistance (Caputo et al., 2020; Jamshidi et al., 2013).
- **Chemical additives**, such as surfactants and emulsifiers, enhance binder-aggregate adhesion by modifying surface energy at the interface. These additives improve mixture workability and compaction without significantly altering binder viscosity (Bairgi et al., 2019; Caputo et al., 2020). Popular chemical additives—including Evotherm, Anova, Rediset, Revix, and Zycotherm—dominate the U.S. market, accounting for approximately 64% of WMA production in 2022 (Williams et al., 2024). In addition, chemical WMA technologies have been shown to support the effective integration of higher levels of recycled materials, further optimizing resource use (Fakhri et al., 2021).

3.2 Benefits of WMA Technology

The adoption of WMA technologies has been driven by both operational efficiency and long-term infrastructure performance goals. Lower production temperatures can result in significant reductions in burner fuel use and improved mixture properties that support pavement durability. The following sections describe these benefits in more detail.

3.2.1 Reducing Fuel Consumption Through Lower Production Temperatures

Lower production temperatures translate directly into reduced burner fuel consumption at asphalt plants. West, Rodezno, Julian and Prowell (2014) reported an average fuel savings of 22.1% based on burner fuel data collected from six different plants, with an average temperature reduction of 48°F when producing WMA mixtures compared to HMA production. Similarly, Sukhija et al. (2022) summarized data from several studies and found that energy savings from WMA production can range from 8% to 40%, depending on factors such as plant configuration, fuel type, production temperature reduction, and the specific WMA technology used. Croteau and Tessier (2008) demonstrated that for each ton of WMA produced, greenhouse gas emissions (GHG) can be reduced by approximately 4.1 to 5.5 kg CO_2 equivalent.

According to the survey by the National Asphalt Pavement Association (NAPA) in 2022, the widespread adoption of WMA in the U.S. reduced emissions by approximately 0.18 million metric tons of CO_2 equivalent, comparable to the annual emissions of about 40,000 passenger vehicles (Williams et al., 2024). These fuel savings not only reduce operating costs but also contribute to more efficient and resilient infrastructure project delivery.

3.2.2 Impacts of Lower Production Temperatures on Asphalt Mixture Performance

In addition to operational efficiencies, WMA technologies can positively influence pavement performance. Lower production temperatures reduce binder aging during mixing and placement, preserving flexibility and improving cracking and fatigue resistance (Dao et al., 2022; Yin, West, et al., 2023). Enhanced workability also makes it easier to achieve target compaction, which is critical to pavement longevity.

However, some performance challenges have been noted. Reduced temperatures may increase moisture susceptibility due to incomplete aggregate drying or lead to potential changes in binder stiffness (Garcia Cucalon et al., 2017; Zaumanis, 2014). While several laboratory studies have reported comparable or improved rutting and cracking resistance for WMA mixtures (Wen et al., 2016), long-term field studies have shown mixed results. For example, studies in Louisiana observed lower fatigue cracking resistance in WMA test sections compared to HMA after five to eight years of service (Akentuna et al., 2022).

Because of these uncertainties, many agencies currently use WMA technologies as compaction aids while maintaining conservative production temperature reductions. Continued field evaluation and advanced mechanistic modeling are essential to support broader implementation and to confirm long-term performance reliability under diverse conditions.

4. METHODOLOGY

4.1 Experimental Plan

This study consisted of two experiments. Experiment 1 evaluated two WMA mixtures (i.e., WMA1 and WMA2, which utilized different WMA technologies) and a control HMA mixture. The planned production temperatures were set at 320-330°F for the HMA and 275-285°F for the WMA mixtures, which could result in an intended target of reducing the production temperature by approximately 50°F. However, on the day of WMA1 production, the contractor was also producing another HMA mixture for a local municipal paving project, with a target production temperature of 300-310°F, and there was an issue with the drag conveyor at the plant. As a result, the target production temperatures for the two WMA mixtures were adjusted to 295-305°F, resulting in a temperature reduction of around 25°F instead of the initially planned 50°F when utilizing the WMA technologies.

During production, data on burner fuel consumption were collected for each mixture. Loose plant mixtures were sampled at the plant and transported to the NCAT laboratory. In addition, the component materials of the mixtures were sampled to conduct a laboratory experiment focused on temperature reduction and advanced performance testing using lab-mixed lab-compacted (LMLC) specimens.

Based on observations and constraints encountered in Experiment 1, Experiment 2 was designed to evaluate the effects of larger temperature reductions following a stepwise approach. This experiment was conducted with a different contractor using the WMA technology utilized in WMA1, and it included one control HMA and one WMA mixture. The control HMA was produced at 320–330°F, while the WMA mixture was produced in incremental temperature steps, starting at 320–330°F and reducing in approximately 10°F intervals down to 260–270°F. Production was scheduled on a day when no other mixtures were being produced at the plant to avoid operational interference.

Fuel consumption data were collected throughout production. Plant mix samples were taken at intermediate (approximately 285°F) and minimum (approximately 260°F) production temperatures and used to prepare hot plant-mixed, lab-compacted (H-PMLC) specimens for rutting and cracking performance evaluation.

Table 1 shows the mix design details of HMA mixtures and the ALDOT specification requirements for each mixture. According to ALDOT specifications, mixtures were compacted at 60 gyrations for Superpave volumetric designs (ALDOT, 2022d). The following sections provide more details for each experiment.

Table 1: Job Mix Formula (JMF) Properties and Acceptance Ranges

Mix Properties	Experiment 1		Experiment 2	
	JMF	ALDOT Limits	JMF	ALDOT Limits
MAS (mm)	12.5	N/A	19.5	N/A
RAP (%)	20	Max 20	20	Max 20
RBR (%)	15.3	N/A	19.6	N/A
Asphalt Content (%)	5.5	Min 5.5	5.1	Min 5.1
Virgin Asphalt Content (%)	4.6	N/A	4.1	N/A
Air Voids (%)	4.0	4.0	4.0	4.0
VMA (%)	16.5	Min 15.5	15.1	Min 14.5
VFA (%)	75.8	N/A	73.5	N/A
D/P_{be}	1.16	0.6-1.4	0.77	0.6-1.4

4.1.1 Plan for Experiment 1

Experiment 1 was conducted at an asphalt plant in Montgomery, Alabama, for an overlay project on US-82 near Prattville. Figure 1 shows the location of the sections that were paved for Experiment 1. Figure 2 shows the plan for this experiment. Three mixtures were planned for this experiment: one control HMA and two WMA mixtures (i.e., WMA1 and WMA2 using different WMA technologies), each produced at a rate of approximately 250 tons per hour. The chemical additives selected for the WMA mixtures were terminal-blended into the virgin binder at a dosage of 0.5% by weight, following the recommendations from the respective WMA suppliers.

a) HMA and WMA1 sections

b) WMA2 section

Figure 1: The sections constructed for Experiment 1

All mixtures were produced with the same aggregate gradation and asphalt content. The gradation was a fine-graded blend with a maximum aggregate size of 12.5 mm and 20% RAP, as shown in Figure 3. The binder was a PG 76-22 modified with 2.5% Styrene-Butadiene-Styrene (SBS) polymer, which meets the ALDOT traffic-based grade bumping requirements (ALDOT, 2022b). Table 2 provides a summary of the design volumetric properties of the mixtures for this experiment. The volumetric results of the mixtures are comparable to those of the JMF.

The HMA mixture was produced first in September 2023, with an average daily ambient temperature of 86.4°F (30.2°C). WMA1 was produced the following day under similar ambient temperature conditions. However, the additive needed for WMA2 did not arrive on time due to a shipment issue, causing a delay in production. As a result, WMA2 was produced in December 2023, with an average daily ambient temperature of 50.7°F (10.4°C), which is approximately 36°F (20°C) lower than that of the HMA and WMA2 production days.

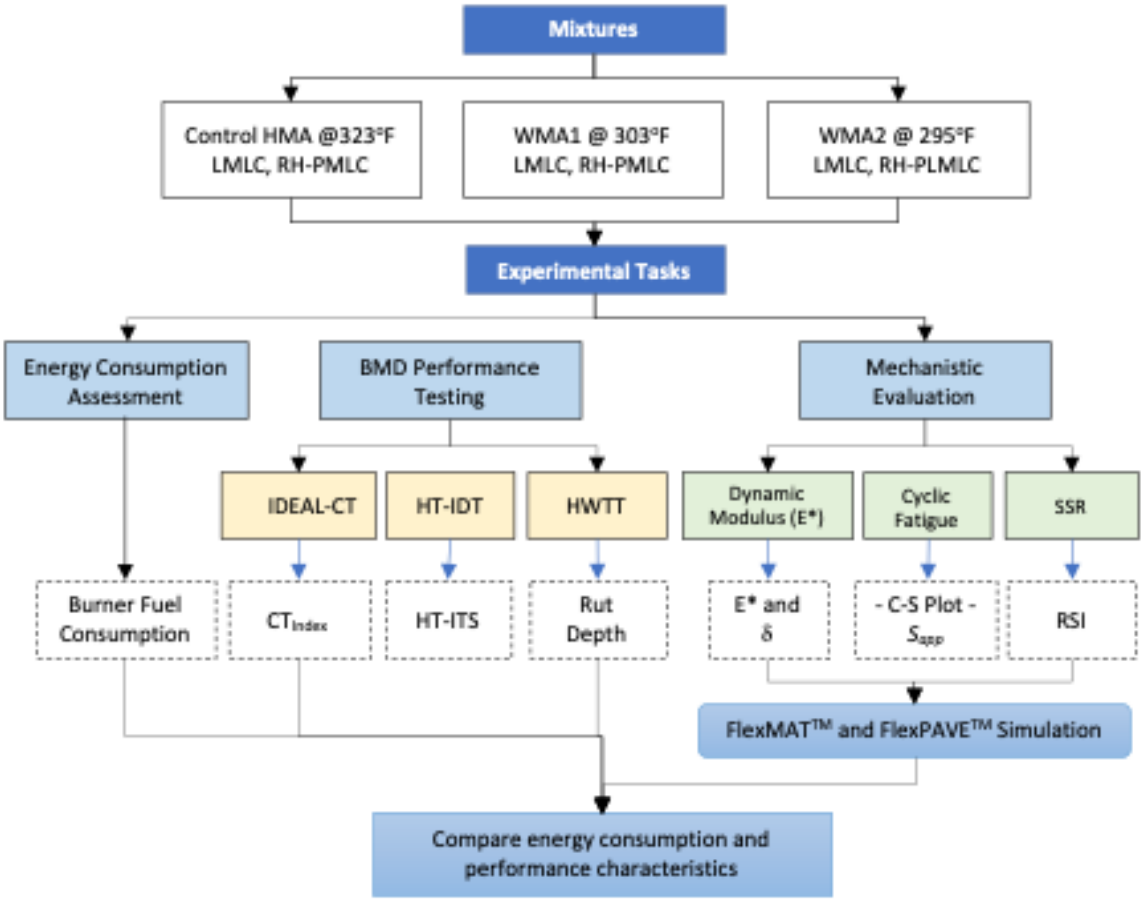

Figure 2. Plan for Experiment 1

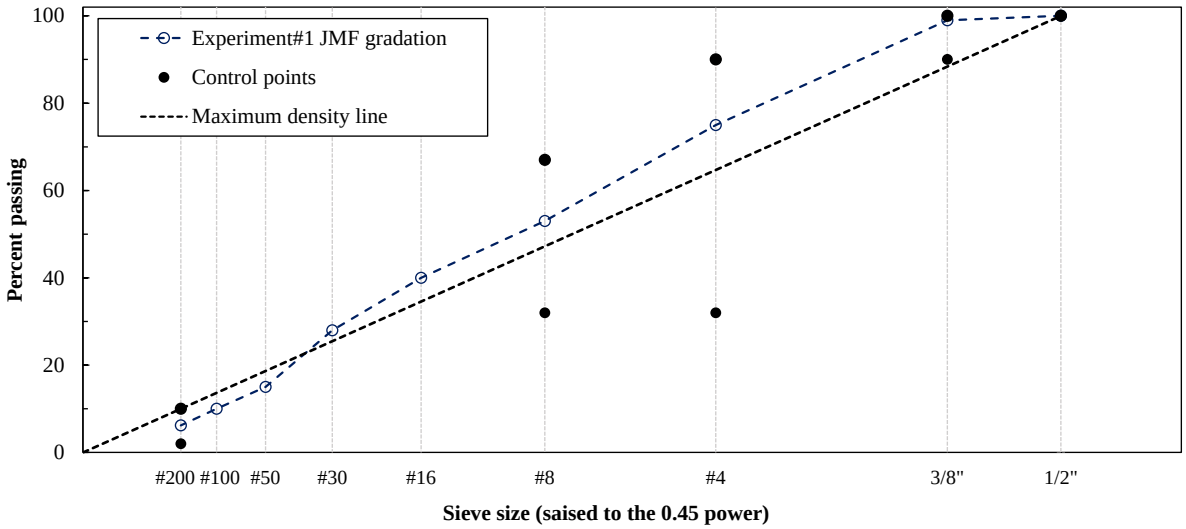

Figure 3. Design aggregate gradation for experiment 1

Table 2: Volumetric Quality Control Data compared to JMF for Experiment 1

Mix Properties	HMA	WMA1	WMA2	JMF
Asphalt Content (%)	5.50	5.53	5.44	5.50
Air Voids (%)	3.96	4.18	3.70	4.17
VMA (%)	16.0	16.6	15.4	16.5
VFA (%)	75.3	74.8	75.9	74.7
D/P_{be}	1.22	1.07	1.15	1.16

Loose mixtures collected from the asphalt plant were reheated in the laboratory and compacted to prepare reheated plant-mixed, lab-compacted (RH-PMLC) specimens for BMD and mechanistic testing, following NAPA IS-145 guidelines (NAPA, 2023). Additionally, component materials sampled from the asphalt plant were used to prepare lab-mixed, lab-compacted (LMLC) specimens at the production temperatures at the originally planned production temperatures (i.e., 320-330°F for HMA and 275-285°F for WMA). After mixing, LMLC samples were short-term aged (STA) for 2 hours at 275°F (135°C) for HMA samples and 240°F (116°C) for WMA samples, as per AASHTO R30-22 (AASHTO, 2023b). To evaluate the sensitivity of WMA mixtures to aging temperature, another set of WMA mixtures was prepared and short-term aged for 2 hours at 275°F (135°C). Table 3 summarizes the mixing, conditioning, and compaction temperatures for the mixtures in Experiment 1. The production temperatures for the control HMA ranged from 320°F to 330°F, with an average of 323°F. For WMA1, the production temperatures ranged from 300°F to 310°F, with an average of 303°F, while the temperatures ranged from 290°F to 300°F, averaging 295°F for WMA2. These results show production temperature reductions of approximately 20°F (11°C) for WMA1 and 28°F (16°C) for WMA2, respectively.

Table 3: Mixing, Conditioning, and Compaction Temperatures used in Experiment 1

Mix Designation	RH-PMLC		LMLC	
	Production Temperature (°F)	Reheating and Compaction Temperature (°F)	Mixing Temperature (°F)	STA and Compaction Temperatures (°F)
HMA	323	275	325	275
WMA1	303	240	275	275 and 240
WMA2	295	240	275	275 and 240

4.1.2 Plan for Experiment 2

While Experiment 1 provided valuable initial insights, the observed limitations in production flexibility suggested the need for a more controlled assessment. Experiment 2 was therefore designed to evaluate the effects of further reducing WMA production temperatures on fuel consumption and performance properties using the additive used in WMA1 in Experiment 1. This experiment was conducted in June 2024 at an asphalt plant in Ariton, Alabama, with the daily ambient temperature measured from 75°F (24°C) in the morning to 88°F (31°C) in the afternoon for the production days. Figure 4 displays the location of the sections for Experiment 2.

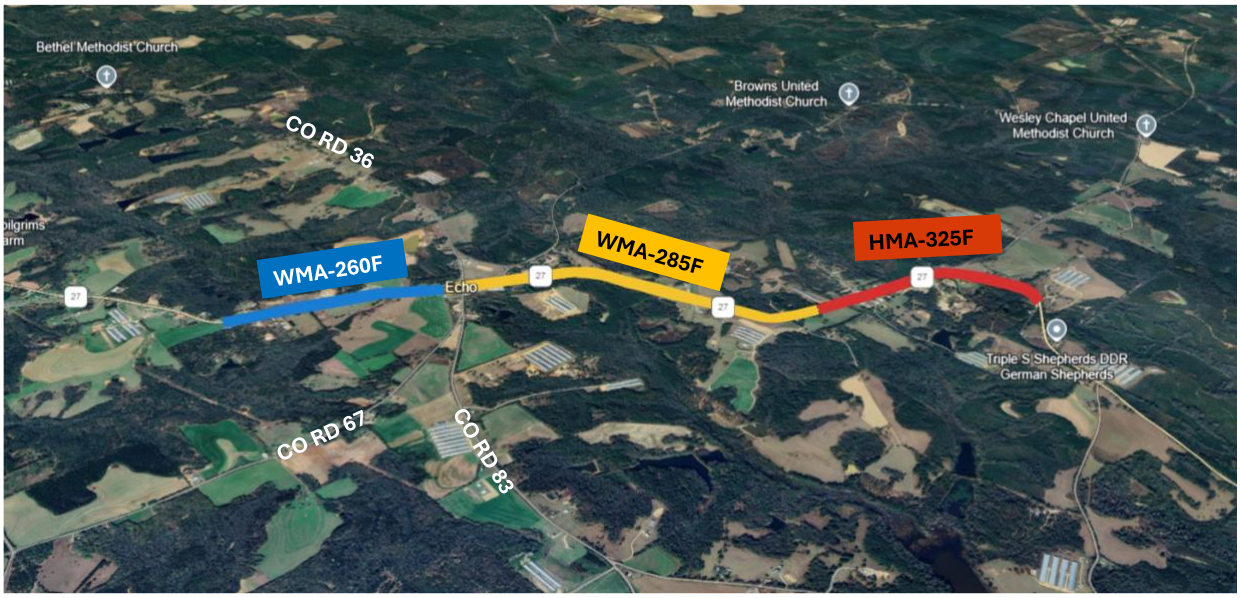

Figure 4: The sections constructed for Experiment 2

In this experiment, a 19 mm MAS mixture containing 20% RAP was used, with a PG 67-22 binder. The control HMA was produced at 325°F (163°C). For WMA production, the binder was terminal-blended with 0.5% WMA additive by weight of the virgin binder, which is the same as in Experiment 1. The WMA mixture was produced in incremental temperature steps, starting at 320–330°F and reducing in approximately 10°F intervals down to 260–270°F. The first sample of the WMA mixture was taken at around 285 °F (141°C) and the second at approximately 260 °F (127 °C). All mixtures were compacted at their target compaction temperatures in a laboratory

at the asphalt plant to prepare hot-compacted, plant-mixed, lab-compacted (H-PMLC) specimens for BMD performance testing, as shown in Figure 5. The design gradation of the produced mixtures is presented in Figure 5, and the production and compaction temperatures for this experiment are shown in Table 4. Asphalt mixtures were also sampled and transported to the laboratory for further evaluation using RH-PMLC specimens.

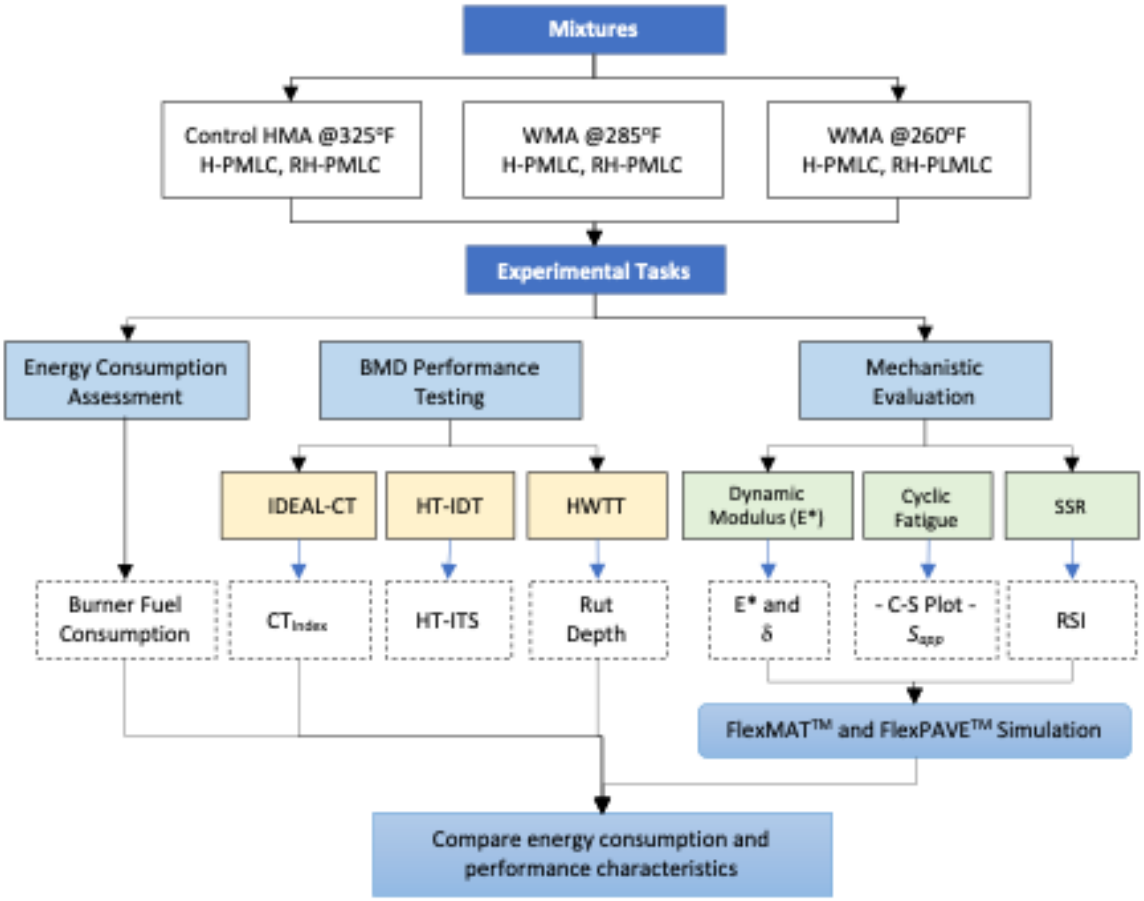

Figure 5. Plan for Experiment 2

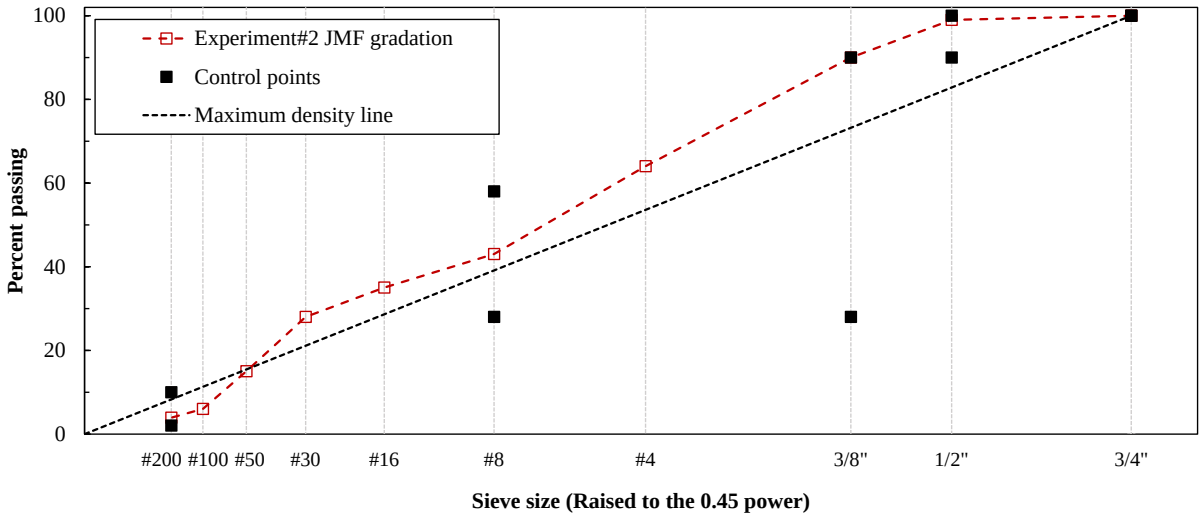

Figure 6. Design aggregate gradation for Experiment 2

Table 4: Mixing and Compaction Temperatures for the Mixtures in Experiment 2

Mix designation	Plant Production Temp (°F)	Compaction temp (°F)
HMA-325F	325	280-290
WMA-285F	285	250-260
WMA-260F	260	230-240

Table 5 presents the quality control volumetric properties of the mixtures produced in Experiment 2. The average air void content and voids in the mineral aggregate (VMA) were slightly lower during production than the JMF targets. The WMA mixtures showed marginally lower air voids and slightly higher voids filled with asphalt (VFA) values compared to the control HMA; however, these differences were minor. No issues were observed during field placement and compaction, indicating that reducing production temperatures with WMA did not adversely affect their volumetric properties or field workability and compaction.

Table 5: Volumetric Quality Control Data for the Mixtures in Experiment 2 compared to JMF

Mix Properties	HMA-325F	WMA-285F	WMA-260F	JMF
Asphalt Content (%)	5.0	5.1	5.1	5.1
Air Voids (%)	3.5	3.4	3.2	4.0
VMA (%)	14.2	14.2	14.4	15.1
VFA (%)	75.6	76.3	77.5	73.5
D/P_{be}	0.7	0.9	0.9	0.8

4.2 Energy Consumption Data Collection and Analysis

Both asphalt plants in this study used No. 2 recycled oil as the burner fuel, stored in on-site cylindrical tanks, and monitored by analog gauges. Burner fuel consumption was recorded in gallons at 30-minute intervals, along with the corresponding asphalt mixture tonnage produced during the 30-minute interval.

These data were used to calculate the amount of burner fuel consumed per short ton of asphalt mixture for each 30-minute interval, using Equation 1. An energy intensity value of 140,000 British thermal units (BTU) per gallon was applied to convert fuel consumption into energy usage per ton of asphalt mixture (Environmental Protection Agency, 2024).

The collected data was then combined for all intervals to calculate the average energy consumption and variability for each asphalt mixture. This approach provided a detailed assessment of production energy consumption and allowed for direct efficiency comparisons between mixtures and production temperatures. It should be noted that energy usage information related to hot oil heaters that are used to heat the asphalt binder was not collected as part of this study.

$$E_i = 140000 \times \frac{V_i}{M_i} \quad \text{Equation 1}$$

where:

E_i = energy consumption during interval *i* (BTU/ton)
V_i = volume of diesel used during interval *i* (gallon)
M_i = tonnage of asphalt mixture produced during interval *i* (ton)

4.3 Laboratory Testing

A comprehensive laboratory testing program was conducted to characterize the recovered binders and asphalt mixtures produced for both field experiments. The objective was to assess key rheological and mechanical properties that influence in-service pavement performance using standard test protocols, advanced performance tests, and pavement analysis tools.

4.3.1 Binder Testing

Binder extraction and recovery were performed on plant-produced asphalt mixture samples in accordance with AASHTO T164-22 (AASHTO, 2024a) and ASTM D5404-24 (ASTM, 2024) procedures. Recovered binders were evaluated using Superpave Performance Grading (PG) protocols as per AASHTO R29-15(2023) and AASHTO M320-23 (AASHTO, 2023a). The continuous high-, intermediate-, and low-temperature grades were determined using Dynamic Shear Rheometer (DSR) and Bending Beam Rheometer (BBR) testing. For the polymer-modified binder in Experiment 1, the Multiple Stress Creep Recovery (MSCR) test was conducted following AASHTO T350-19(2023) (AASHTO, 2023f) and AASHTO M323-22 (AASHTO, 2022a), providing additional insight into elastic recovery and rutting susceptibility.

4.3.1.1 Performance Grading (AASHTO M320)

High- and intermediate-temperature performance grades (PG) were determined using the DSR according to AASHTO T315 (AASHTO, 2024b). Since plant-produced mixtures undergo significant

short-term aging during production, RTFO aging was not conducted on the recovered binders. The DSR applied a sinusoidal torsional shear stress to measure the complex shear modulus (|G*|) and phase angle (δ). The high-temperature grade was determined by the maximum temperature at which the binder can still maintain a minimum |G*|/sin δ value of 2.2 kPa, as per AASHTO T315. Continuous grading was calculated by interpolating between the passing and failing temperatures, as per ASTM D7643-22 (ASTM, 2022).

Intermediate-temperature grading was determined by subjecting the extracted binder to 20 hours of long-term aging in a pressure aging vessel (PAV), followed by DSR testing as per AASHTO T 315. The grade was determined by finding the highest temperature at which the |G*| × sin δ parameter reached or exceeded 6000 kPa in accordance with AASHTO M320. Additionally, the continuous grading was calculated by interpolating the passing and failing temperatures for the exact threshold value, as per ASTM D7643-22.

Low-temperature performance grades were determined using the Bending Beam Rheometer (BBR), conducted on PAV-aged binders as per AASHTO T313-22 (AASHTO, 2022b). The BBR test measured creep stiffness (S) and the rate of stress relaxation (m-value). The low-temperature grade was determined based on the warmer of the two temperatures where the S-value reaches a maximum of 300 MPa or the m-value meets a minimum of 0.300.

4.3.1.2 Multiple Stress Creep Recovery (MSCR) Test

The MSCR test was performed to further characterize the polymer-modified binder used in Experiment 1 in accordance with AASHTO T350-19(2023). This test provides an assessment of the binder's ability to recover from applied stresses and is particularly relevant for evaluating rutting resistance in polymer-modified binders. Testing was conducted using a DSR equipped with 25 mm parallel plates and a 1 mm gap. The test sequence included the application of 10 creep-recovery cycles at two stress levels: 0.1 kPa and 3.2 kPa. Each cycle consisted of a one-second creep load followed by a nine-second recovery period.

Two key parameters were calculated: non-recoverable creep compliance (J_{nr}) and the change in compliance from the two stress levels ($J_{nr,diff}$). Lower J_{nr} values indicate stiffer binders with improved rutting resistance. Testing was conducted at 64°C, which corresponds to the environmental high PG grade for the project location. As with other binder tests, RTFO aging was not conducted, as the production process had already imparted sufficient short-term aging.

4.3.2 BMD Performance Testing

To evaluate the cracking and rutting resistance of the asphalt mixtures, BMD performance tests were conducted. These included the Indirect Tensile Asphalt Cracking Test (IDEAL-CT), Hamburg Wheel-Tracking Test (HWTT), and the High-Temperature Indirect Tensile Test (HT-IDT). These tests were selected by ALDOT to implement BMD specifications.

4.3.2.1 Indirect Tensile Asphalt Cracking Test (IDEAL-CT)

The IDEAL-CT was conducted at 25°C using a minimum of four cylindrical specimens. Each specimen was preconditioned for two hours in an environmental chamber prior to testing. The test involves loading the specimen in compression along its vertical diameter, thereby inducing indirect tensile stress (Zhou et al., 2017).

Figure 7 shows a typical IDEAL-CT specimen in the test frame used in this study. The specimens were 150 mm in diameter and 62 mm in height, compacted to achieve target air voids of 7 ± 0.5%, in accordance with ASTM D8225-19 (ASTM, 2019). During the test, a monotonic load was applied to the specimen at a constant displacement rate of 50 mm/min until failure.

The measure of cracking performance, the CT_{index}, is calculated based on the failure energy, slope, and displacement at 75% of the post-peak load, and the thickness and diameter of the specimen (Equation 2). CT_{index} is the resulting parameter from the IDEAL-CT test to characterize the cracking properties of the mixture. A higher value of CT_{index} is desired for better cracking resistance.

$$CT_{index} = \frac{t}{62} * \frac{G_f}{|m_{75}|} * \frac{L_{75}}{D} \quad \text{Equation 2}$$

Where:

G_f = failure energy (J/m^2)
m_{75} = slope at 75% of post-peak load (kN/mm)
l_{75} = displacement at 75% post-peak load (mm)
t = thickness of sample (mm)
D = specimen diameter (mm).

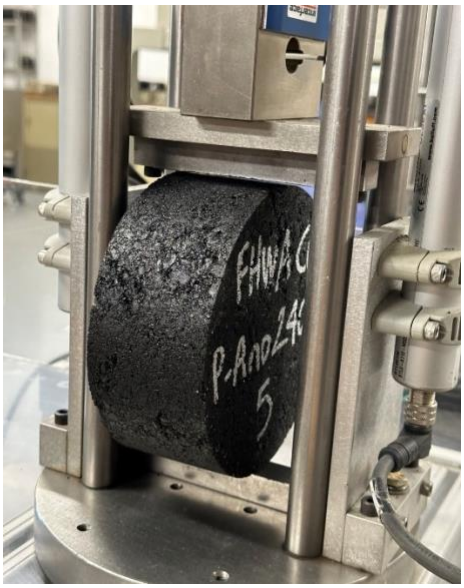

Figure 7: The IDEAL-CT Setup

4.3.2.2 Hamburg Wheel-Tracking Testing (HWTT)

The HWTT test, as per AASHTO T324-23 (AASHTO, 2023e), is widely utilized in asphalt mix design to assess mixture resistance to rutting and moisture damage. In the HWTT, a 158-lb steel wheel moves back and forth across a pair of asphalt specimens submerged in water at a rate of 52 ± 2 passes per minute, simulating repeated traffic loading. In this study, testing was conducted at 50°C. All specimens were compacted at an air void content of 7±0.5%.

The test records the accumulated deformation at each loading cycle. The deformation plot as a function of loading cycles was analyzed for rutting and moisture resistance. The plot typically consists of three phases: post-compaction, creep, and stripping. The post-compaction phase reflects the initial consolidation of the specimen, usually occurring within the first 1,000 passes. The creep phase involves a nearly constant rate of deformation due to visco-plastic flow, starting after the post-compaction phase. The stripping phase begins when the asphalt binder-aggregate bond starts to degrade, leading to moisture damage initiation. As the final output, the total rut depth is used as the rutting resistance. Figure 8 shows the laboratory setup of HWTT testing.

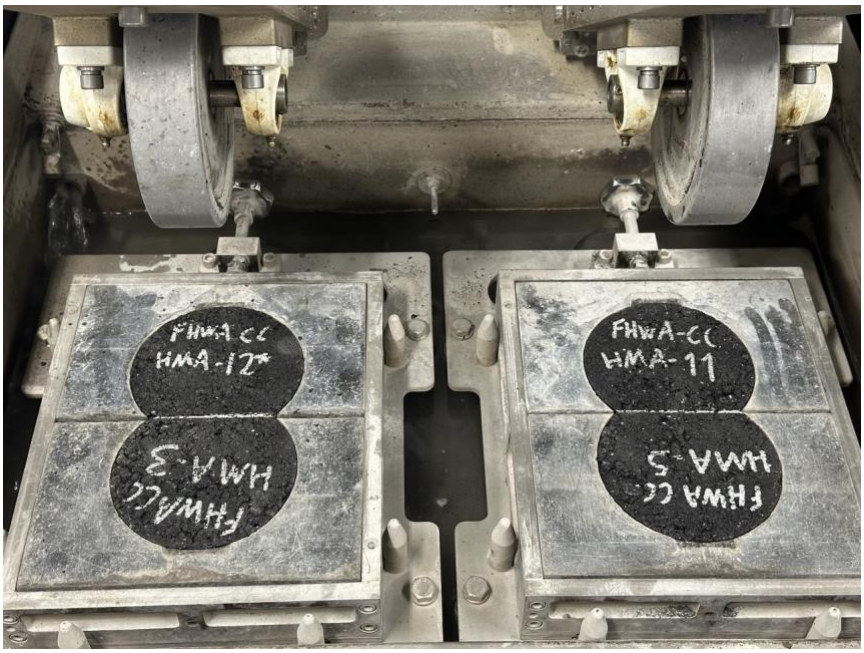

Figure 8: The HWTT Setup

4.3.2.3 High-Temperature Indirect Tensile Test (HT-IDT)

The HT-IDT test, as per ALDOT 458 (ALDOT, 2022a), is an indirect tensile strength (ITS) test performed at a constant loading rate of 50 mm/min. The only difference is that it is conducted on specimens conditioned at a higher temperature rather than 25°C. Typically, the test is carried out at the high temperature experienced by the pavement in service. Alternatively, the high-performance grade (PG) temperature of the binder can also be used. For each mix, four 150mm by 62mm gyratory specimens at 7±0.5% air voids were conditioned for one hour in a water bath set to 50°C and tested. The resulting parameter is the high-temperature ITS (HT-ITS), and a higher value is desired for better resistance to rutting. Figure 9 shows an HT-IDT test specimen in the test frame.

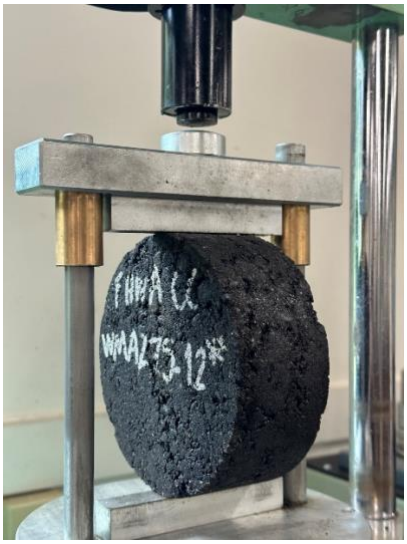

Figure 9: The HT-IDT Setup

4.3.3 Performance Testing using AMPT

The study includes a mechanistic performance evaluation of the mixtures using several advanced performance tests conducted using an Asphalt Mixture Performance Tester (AMPT), including the dynamic modulus (|E*|), cyclic fatigue, and stress sweep rutting (SSR). These test results are analyzed to provide input parameters for asphalt pavement performance modeling. **Figure *10*** shows the IPC Global© AMPT and AMPT Pro utilized to conduct AMPT tests in this study.

Figure 10: The AMPT used for |E*| and Cyclic Fatigue Tests

4.3.3.1 Dynamic Modulus Test

The |E*| test is used to evaluate the stiffness and viscoelastic behavior of asphalt mixtures. Specimens with both large-scale (100 mm in diameter and 150 mm in height) and small-scale (38

mm in diameter and 110 mm in height) geometries can be tested. This study conducted the test on small specimens using an AMPT following AASHTO TP132-23 (AASHTO, 2023d). Small-scale specimens compacted to an air void content of 7.0±0.5% were prepared by coring and sawing from a Superpave Gyratory Compactor (SGC) specimen. The test was conducted at three different temperatures (4°C, 20°C, and 40°C) and three loading frequencies (10 Hz, 1 Hz, and 0.1 Hz) at each temperature. Figure 10 shows the IPC Global© AMPT utilized to conduct the dynamic modulus tests in this study. Figure 11 shows small AMPT specimens utilized for the dynamic modulus test in this study.

Figure 11: Small Scale AMPT Specimens

During the test, the specimen is subjected to sinusoidal compressive loading, which causes axial peak-to-peak strains in the target range of 70 to 75 microstrains. These stress-strain data are then analyzed to calculate the dynamic modulus, the ratio of peak stress to peak strain at a given temperature and frequency. In addition, the phase angle, the time lag between stress and strain peaks, is also determined to assess the viscoelastic properties. Dynamic modulus and phase angle were used as input parameters for FlexPAVE™ modeling.

They were also analyzed using the time-temperature superposition principle to develop a dynamic modulus master curve, which helped better interpret the stiffness properties of the mixtures at varying temperatures and frequencies. In accordance with AASHTO R84-17(21) (AASHTO, 2021), Master Solver for Excel© Version 2.3 was utilized to produce dynamic modulus and phase angle master curves. Within the software, the dynamic modulus master curve was developed based on a sigmoidal form shown in Equation 3.

$$log|E^*| = \log(Min) + \frac{(\log(Max) - \log(Min))}{1 + e^{\beta + \gamma log \omega_r}} \quad \text{Equation 3}$$

Where:

$|E^*|$ = dynamic modulus, ksi
ω_r= reduced frequency at the reference temperature, Hz
Max= Limiting maximum modulus, ksi
Min= Limiting minimum modulus, ksi
β and γ= Fitting parameters

The reduced frequency is calculated using the Arrhenius equation shown in Equation 4.

$$log\omega_r = log\omega + \frac{\Delta E_a}{19.14714}\left(\frac{1}{T} - \frac{1}{T_r}\right) \quad \text{Equation 4}$$

Where:

ω_r= Reduced frequency at the reference temperature, Hz
ω= Reduced frequency at the test temperature, Hz
$T_r =$ Reference temperature, °K
$T =$ Test temperature, °K
$\Delta E_a =$ Activation energy (treated as a fitting parameter)

In addition, the mixture Glover-Rowe (G-R_m) parameter was calculated for the mixtures using the |E*| and δ data to assess the cracking resistance of asphalt mixtures. Similar to its origin in asphalt binders, G-R_m is calculated using Equation 5, where lower values indicate better resistance to cracking. In this study, the G-R_m parameters were calculated using a temperature-frequency combination of 20 °C and 5 Hz, as recommended in the literature (Oshone et al., 2019; Zhang et al., 2022).

$$G\text{-}R_m = \frac{|E^*|(\cos(\delta))^2}{\sin(\delta)} \quad \text{Equation 5}$$

4.3.3.2 Cyclic Fatigue Test

The AMPT cyclic fatigue test, in accordance with AASHTO T411-24 (AASHTO, 2024c), is conducted to determine the damage characteristic curve and evaluate the fatigue resistance of asphalt mixtures. The simplified viscoelastic continuum damage (S-VECD) model is used to analyze the data. This study used small-scale specimens (38 mm in diameter and 110 mm in height) with 7 ± 0.5% air voids in this test. In accordance with AASHTO T411-24, the test was run using an axial gauge length of 70 mm at the temperature and frequency of 21°C and 10Hz, respectively. The test is conducted at appropriate strain rates so that the failure occurs between 2,000 and 80,000 cycles. The range of strain rates employed to achieve appropriate results for the first and second experiments were 450-475 microstrains and 375-450 microstrains, respectively. Key outputs from the test include the pseudo secant modulus versus damage curve, known as the damage characteristic curve, and the pseudo energy-based fatigue failure criterion (D^R). These

fundamental material properties are independent of temperature, frequency, and loading mode effects and are essential for predicting fatigue performance.

The damage characteristic curve defines the mixture's integrity (pseudo stiffness) at various stages of internal damage, while the D^R criterion represents the mixture's toughness, indicating the amount of pseudo energy it can withstand before failure. Both of these properties are used to calculate the cyclic fatigue index (Sapp) parameter, which quantifies the mixture's fatigue resistance. A higher Sapp value suggests better fatigue performance. The test is performed at specified temperatures based on the binder performance grade. Along with the dynamic modulus data, the results are processed using the Federal Highway Administration's FlexMAT™ v2.2 software, which reports the D^R and Sapp parameters and provides the input for FlexPAVE™ v2.2 (Federal Highway Administration, 2025).

4.3.3.3 Stress Sweep Rutting (SSR) Test

The SSR test, specified in AASHTO TP 134-22 (AASHTO, 2022c), evaluates the rutting resistance of asphalt mixtures under simulated traffic load conditions. It measures permanent deformation as a function of deviatoric stress, loading duration, and temperature, offering valuable insights into the mixture's ability to resist rutting.

Following AASHTO TP 134-22, the test was conducted at two temperatures—low (TL) of 26.2°C and high (TH) of 51.2°C—determined based on the pavement's geographic location. As presented in Figure 12, cylindrical specimens with 100 mm in diameter and 150 mm in height were used in this test. A 7 ± 0.5% air void content was maintained in all the specimens. A constant confining pressure of 69 kPa was maintained throughout the test. Each test involves three 200-cycle loading blocks applied at deviatoric stress levels of 483, 689, and 896 kPa for TL and 689, 483, and 896 kPa for TH. Each loading cycle consists of a 0.4-second pulse, followed by periods of 1.6 seconds for TL and 3.6 seconds for TH. Permanent axial deformation was recorded using actuator displacement.

Figure 12: The SSR Test Specimens

Using a permanent deformation shift model, the results from two SSR tests at each temperature were used to characterize the mixture's deformation behavior using FlexMAT™. The model integrated into the FlexPAVE™ enables the prediction of long-term rutting performance under varying stress levels, loading durations, and temperatures as a function of pavement depth and time.

Additionally, the FlexPAVE™ was utilized to calculate the Rutting Strain Index (RSI), a key parameter for evaluating rutting susceptibility. RSI represents the average permanent strain and is calculated by dividing the permanent deformation of an asphalt layer by its thickness after 20 years of traffic loading. This period assumes 30 million repetitions of an 18-kip standard equivalent single axle load (ESAL). Lower RSI values indicate higher rutting resistance.

4.4 Pavement Modeling using FlexPAVE™

FlexPAVE™ is a pavement analysis tool designed to assess the long-term behavior of asphalt pavements under varying material properties, climate conditions, traffic loads, and structural configurations. It utilizes three-dimensional viscoelastic finite element analysis to simulate moving loads and temperature variations over time through pavement depth for calculating stresses and strains (Wang et al., 2021).

These pavement responses are applied to damage models to estimate fatigue cracking and rutting. Fatigue predictions are based on the cyclic fatigue test and the Simplified Viscoelastic Continuum Damage (S-VECD) model (Eslaminia & Guddati, 2016), while rutting predictions rely on the SSR test and a permanent strain shift model (Ghanbari et al., 2022). Studies have shown that FlexPAVE™ predictions correspond well with field observations, particularly in ranking the severity of cracking and rutting (Ghanbari et al., 2022; Wang et al., 2016). The tool provides a link between laboratory material properties and field performance for pavement design and evaluation.

In this study, FlexPAVE™ v2.2 was utilized to evaluate the potential effects of lowered production temperatures on pavement fatigue and rutting performance. The analysis included representative pavement structures, traffic loading scenarios, and climate conditions specific to the project location. Model inputs were obtained from a comprehensive laboratory testing program conducted on the plant mixtures collected during field experiments.

4.4.1 Pavement Structure and Layer Properties

To predict and compare the long-term performance of the asphalt mixtures, a three-layer pavement structure was used in the FlexPAVE™ v2.2 simulations, as presented in Figure 13. This structure represents a representative pavement section used in field project locations, consisting of a 5-inch asphalt layer over a 6-inch soil aggregate base and a 12-inch improved roadbed. Resilient modulus values of 16,000 psi for soil aggregate base and 8,000 psi for roadbed were assigned, as shown in Figure 13. These layer thicknesses and modulus values were selected based on the ALDOT pavement design manual and the recommendations of ALDOT engineers.

Asphalt layer properties specific to each mixture were derived from laboratory testing, including E*, cyclic fatigue, and SSR results processed through FHWA's FlexMAT™ v2.2. The properties of the unbound layer remained consistent across all simulations in both experiments, enabling

direct comparisons between mixtures regarding their effect on the predicted performance of the pavement cross-section.

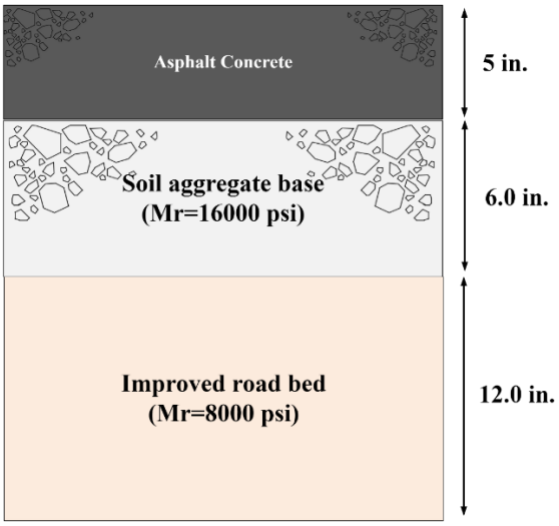

Figure 13. Representative pavement Cross Section used for modeling

4.4.2 Modeling Input Parameters

Modeling parameters were tailored to conditions at the project site along US-82 near Prattville, Alabama. These included geographic location, elevation, water table depth, and climate data from the nearest MERRA2 station to capture site-specific environmental influences. Traffic loading inputs were based on ALDOT's traffic analysis and materials report for the project. A single-axle, dual-tire configuration was used, consistent with the capabilities of FlexPAVE™ v2.2. The key traffic and loading inputs are summarized in Table 6.

Table 6: Input parameters used for pavement modeling

Input parameter	FlexPAVE™ input value
Design life (years)	20
Axle load (kips)	18
Axle load repetitions (Axles per day)	765
Tire pressure (psi)	120
Velocity (mph)	50

4.4.3 Aging Analysis and Modeling Outputs

FlexPAVE™ v2.2 incorporates pavement aging effects using the asphalt mixture aging model developed under NCHRP Project 09-54 (Kim et al., 2021). The model supports three levels of input (i.e., Level I, II, and III), with Level I requiring the most detailed information. In this study, Level III aging inputs were used as follows. The model outputs included two key performance metrics: predicted percent fatigue damage and rut depth progression over time.

- Reclaimed Asphalt Pavement (RAP) content
- Recycled Binder Ratio (RBR)
- High-temperature PG of RAP extracted binder and virgin binder

5. RESULTS AND DATA ANALYSIS

This section presents results and discussions in five parts: (i) burner fuel consumption, (ii) binder rheological testing, (iii) mixture BMD performance testing, (iv) AMPT performance testing, and (v) FlexPave™ pavement analysis. Where appropriate, statistical analysis was conducted using Tukey's Honestly Significant Difference (HSD) test with a one-way Analysis of Variance (ANOVA) at a 0.05 significance level ($\alpha = 0.05$). The assumptions of normality and homogeneity of variances were verified using the Anderson-Darling Normality Test and Levene's test, respectively. Statistical groupings are indicated in figures by letters, where mixtures not sharing the same letters are statistically different. For figures that include both RH-PMLC and LMLC samples, lowercase letters denote groupings for RH-PMLC samples, while uppercase letters represent groupings for LMLC samples.

5.1 Burner Fuel Consumption Results

Figure 14 shows the average burner fuel consumption measured during the production of mixtures in Experiment 1, with error bars representing one standard deviation. The results indicate that energy consumption across all mixtures was generally similar, as confirmed by statistical groupings denoted by letters in the figure. The slightly lower average fuel consumption for WMA1 can be attributed to the average production temperature reduction of around 20°F under similar ambient conditions. Additionally, for WMA2, while the average production temperature was reduced by approximately 28°F compared to that of HMA, which would reduce burner fuel consumption, the average daily ambient temperature on the WMA2 production day was approximately 36°F lower than those during the HMA and WMA1 production days, which may have increased burner fuel consumption. These opposite effects may have resulted in similar burner fuel consumption for HMA and WMA2, as shown in Figure 14.

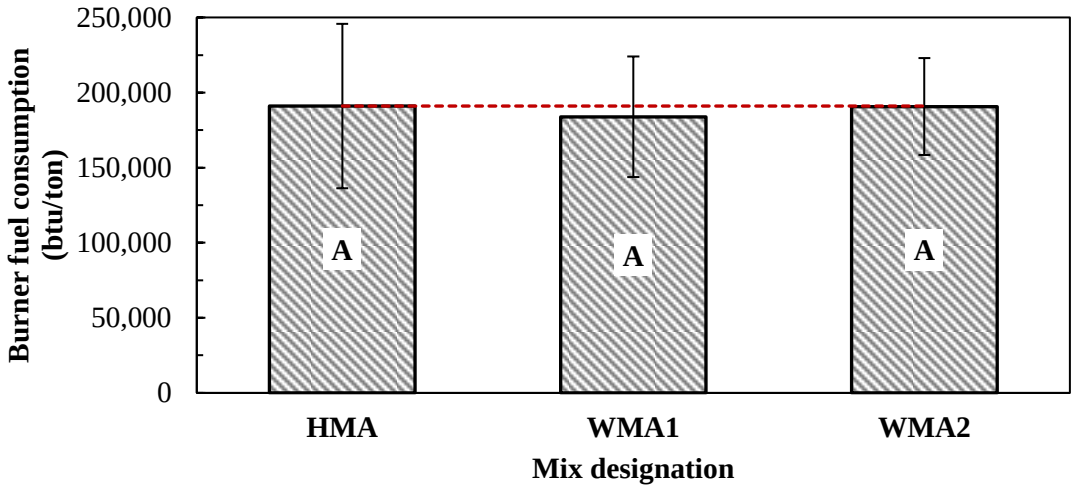

Figure 14. Average burner fuel consumption for the mixtures in Experiment 1

Figure 15 presents the results of burner fuel consumption measured from Experiment 2. The data show that reducing production temperature led to an average energy savings of 8% at 285°F and 19% at 260°F, compared to the control HMA produced at 325°F. Statistical analysis confirmed that fuel consumption for WMA produced at 260°F was significantly lower than that of the control mixture. Additionally, the reduction in energy consumption followed a non-linear pattern, with more pronounced savings at lower temperatures. These findings highlight the importance of achieving sufficient temperature reductions to maximize fuel savings when using WMA technologies.

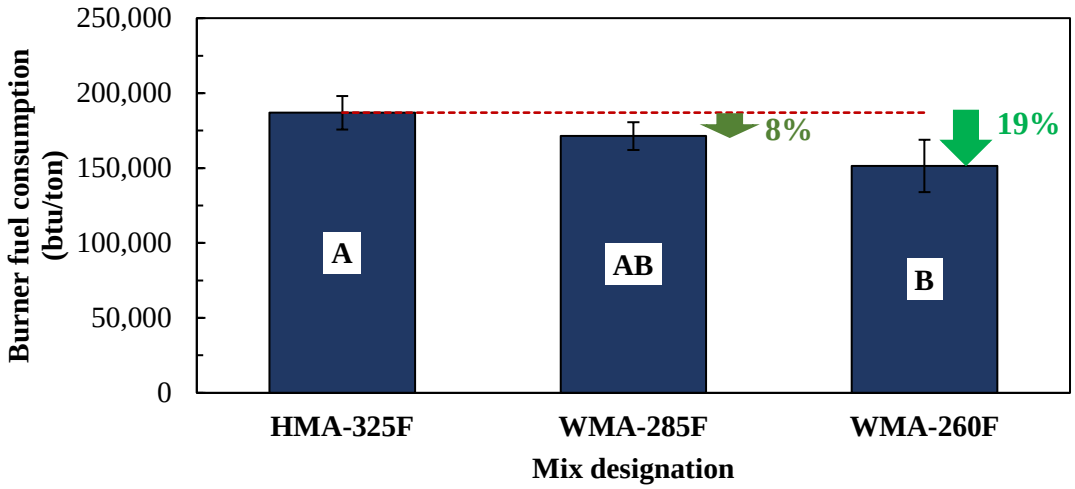

Figure 15. Average burner fuel consumption for the mixtures in Experiment 2

5.2 Asphalt Binder Rheological Properties

Figure 16 and Figure 17 present the continuous performance grading results for high, intermediate, and low temperatures for binders extracted from the plant mixtures in Experiments 1 and 2, respectively. In Experiment 1, binders extracted from the WMA mixtures showed slightly lower high-temperature continuous grades compared to the binder extracted from the control HMA, indicating reduced stiffness and higher phase angles in high-temperature DSR tests. This suggests slightly reduced rutting resistance for WMA binders, likely due to lower production temperatures resulting in lower aging levels. At intermediate temperatures, binders extracted from the WMA mixtures also exhibited lower continuous grades, implying reduced fatigue performance. However, the low-temperature performance results were mixed: the WMA1 binder displayed a lower low-temperature continuous grade, indicating improved performance, while WMA2 showed a higher low-temperature continuous grade, suggesting reduced performance. However, the differences were minimal.

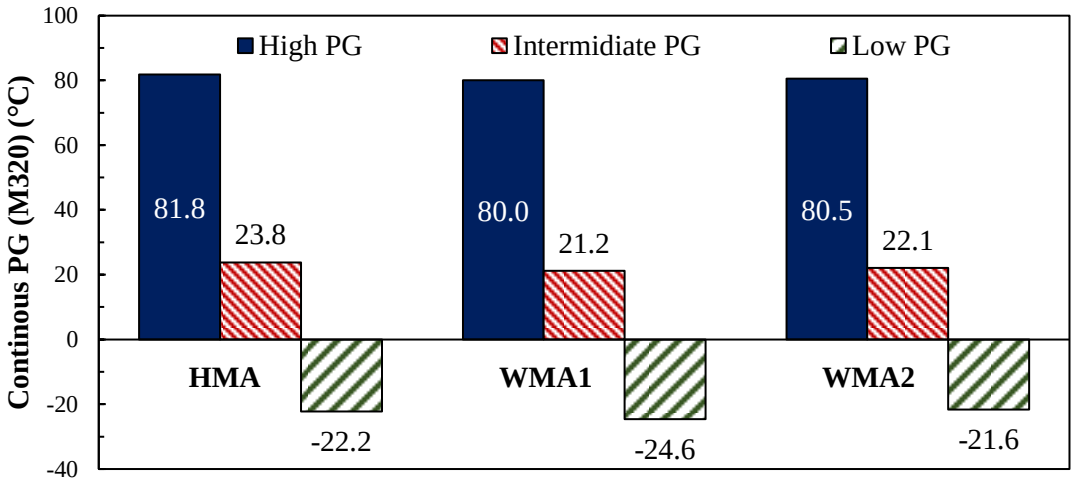

Figure 16. Continuous PG grades of extracted binder in Experiment 1

In Experiment 2, binders extracted from the WMA mixtures demonstrated a larger reduction in high-temperature continuous grades compared to Experiment 1, which can be attributed to larger reductions in production temperature. However, the intermediate continuous grades increased, indicating an improved DSR fatigue index. At low continuous grades, binders extracted from the WMA mixtures exhibited a slight increase in grade, pointing to a slighltly reduction in low-temperature cracking resistance.

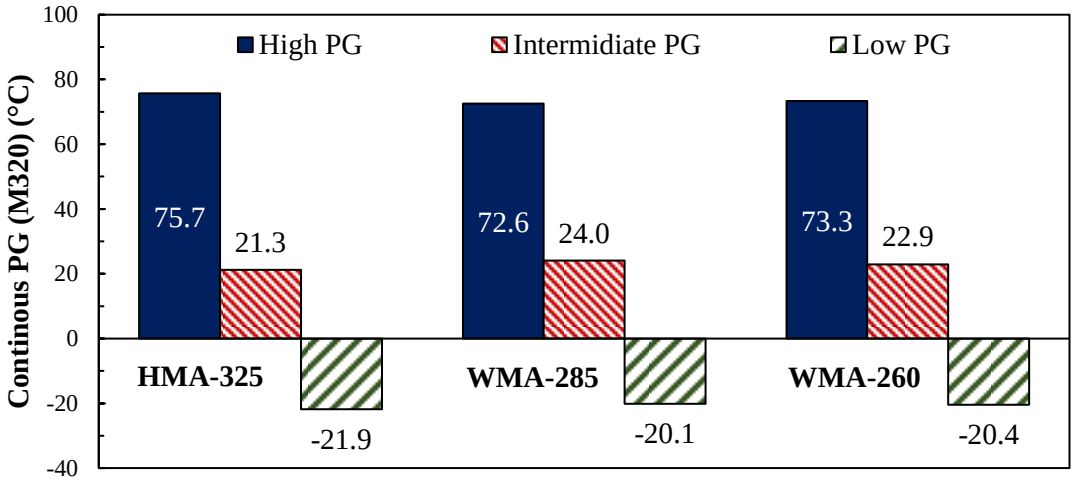

Figure 17. Continuous PG grades of extracted binder in Experiment 2

MSCR test results for binders extracted from the mixtures in Experiment 1, as shown in Figure 18, can be used to assess rutting susceptibility at high service temperatures. The binder extracted from the control HMA had a lower $J_{nr3.2}$ value than those of the WMA1 and WMA2 mixtures, indicating better rutting resistance. However, all values remained below the AASHTO M332-23 threshold of 0.5 kPa^{-1} for level "E" traffic, indicating good rutting resistance. Additionally, the binder extracted from the HMA mixture showed a lower Jnr_{diff} compared to binders extracted from the WMA mixtures, suggesting reduced stress sensitivity for the control HMA.

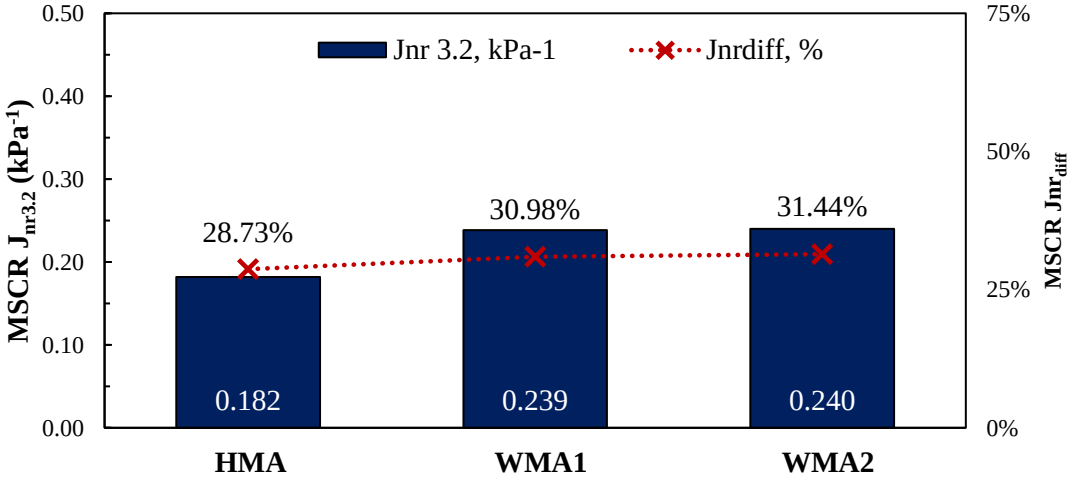

Figure 18. MSCR test results for the extracted binder in Experiment 1

5.3 Mixture BMD Performance Tests

5.3.1 IDEAL-CT Results

Figure 19 presents the average CT_{Index} values from four to six replicate specimens for RH-PMLC and LMLC mixtures in Experiment 1, with error bars representing one standard deviation. While LMLC mixtures were aged under one STA condition (i.e., 2 hours at 275°F), LMLC WMA mixtures were aged under two STA conditions: 2 hours at 275°F (similar to the control HMA) and 2 hours at 240°F, following AASHTO R30-22 guidelines for WMA mixtures.

The maximum and average coefficients of variation (COV) for CT_{Index} for all RH-PMLC and LMLC specimens were 20.4% and 13.3%, respectively. Statistical analysis of all RH-PMLC mixtures in Figure 19 showed no significant differences in CT_{Index} values between mixtures (Group ‘a’), indicating that plant-produced WMA mixtures exhibited cracking resistance comparable to the control HMA. For LMLC mixtures, those aged at 275°F showed no statistical improvement in CT_{Index} values over the control mixture (Group ‘BC’). However, at a lower STA temperature of 240°F, WMA mixtures demonstrated enhanced CT_{Index} values, with WMA1 showing a statistically significant improvement (Group 'A').

These findings suggest that lower production temperatures can enhance the cracking resistance of WMA mixtures. Additionally, the results highlight the significant impact of STA temperature on the cracking resistance of WMA mixtures.

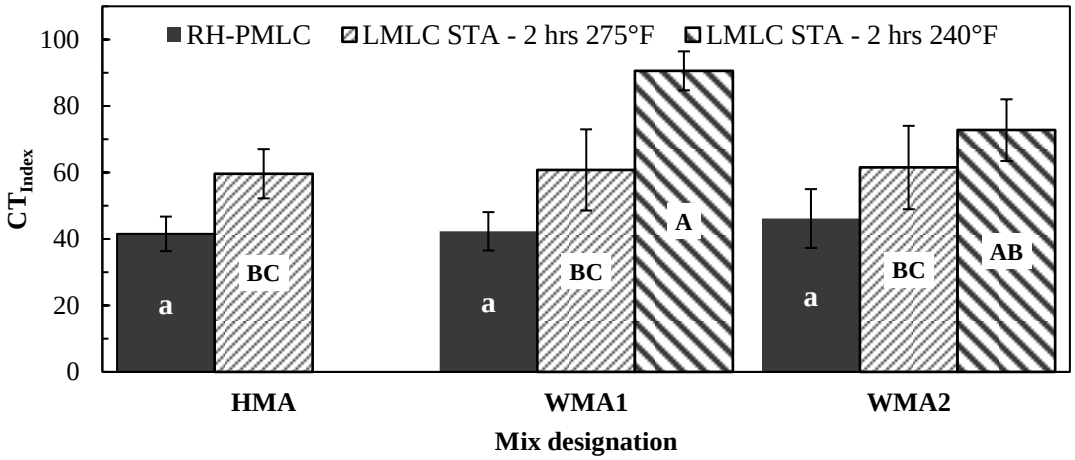

Figure 19. CT_{Index} results for the mixtures in the Experiment 1

To better understand the factors influencing CT_{Index} values, an IDEAL-CT interaction diagram was created by plotting average failure energy against l75/m75 values, with contour lines representing CT_{Index} levels (Yin, Chen, et al., 2023; Yin, West, et al., 2023). In this diagram, failure energy reflects mixture toughness, while l75/m75 represents the ductile-brittle behavior of the mixture. Higher values for both parameters lead to an increase in CT_{index} or cracking performance improvement, shifting the mix towards the upper right corner of the diagram. Figure 20 shows an interaction diagram for the mixtures in Experiment 1. For RH-PMLC specimens, WMA mixtures had lower failure energy but higher l75/m75 compared to the control mixture. The competing effects resulted in similar CT_{Index} values. Among LMLC mixtures, a significant increase in l75/m75 without significant changes in failure energy led to higher CT_{Index} values, indicating that lower STA temperatures improve the mixture's ability to resist cracking by enhancing ductility.

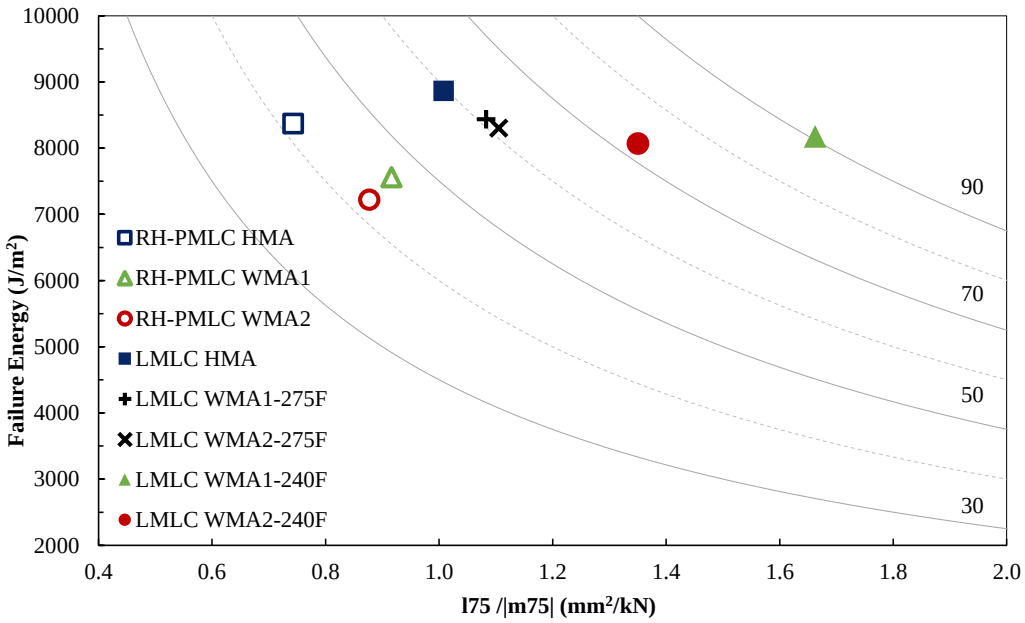

Figure 20. IDEAL-CT interaction plot for the mixtures in Experiment

Figure 21 presents the average CT_{Index} of four replicates for each mixture in Experiment 2. The maximum and average COV were 19.6% and 18.4%, respectively. WMA mixtures produced at 285°F and 260°F had comparable CT_{Index} values, which were similar to that of the control HMA produced at 325°F. This observation suggested that significant temperature reductions did not affect cracking resistance in this experiment. Slight decreases in failure energy and small increases in l75/m75 were observed in WMA mixtures, but these differences were not statistically significant. The average failure energy for WMA produced at 285°F and at 260°F decreased from 6,881.3 J/m² (HMA) to 6,221.2 and 6,441.4, respectively, while l75/m75 increased from 1.623 mm²/kN (HMA) to 1.642 and 1.682, respectively. These findings differ from the LMLC IDEAL-CT results of Experiment 1, indicating that factors beyond production temperatures, such as extended silo storage times at various production temperatures, may affect CT_{Index} values of the plant-produced mixtures.

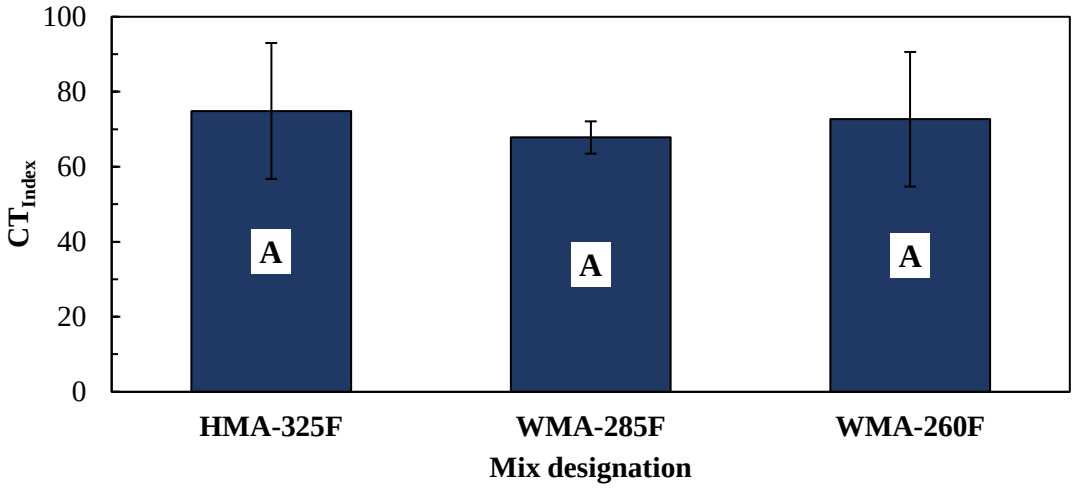

Figure 21. CT_{Index} results for H-PMLC specimens in Experiment 2

5.3.2 HWTT Results

Figure 22 and Figure 23 show the HWTT rut depth results versus the number of passes for RH-PMLC and LMLC samples, respectively. For RH-PMLC specimens, both WMA mixtures exhibited increased rut depths compared to the control HMA, as shown in Figure 22, indicating lower rutting resistance. Additionally, WMA mixtures showed signs of a stripping phase in the rut depth curves, suggesting greater moisture susceptibility. Despite these differences, all mixtures showed rut depths below 5 mm after 20,000 passes, indicating good rutting resistance.

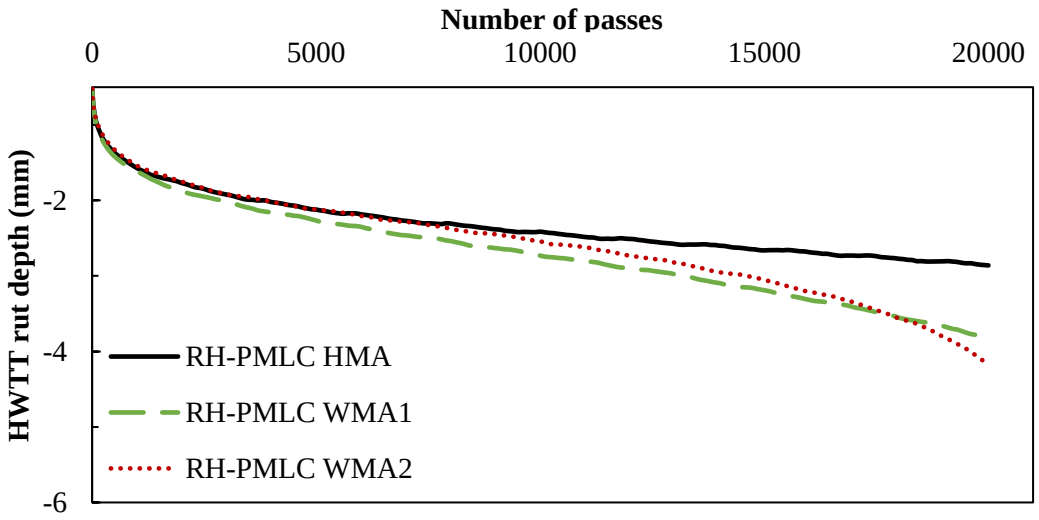

Figure 22. Average HWTT rut depth for RH-PMLC mixtures in Experiment 1

For LMLC specimens (Figure 23), WMA mixtures short-term aged at 275°F exhibited rut depths comparable to the control HMA. However, reducing the STA temperature to 240°F decreased mixture stiffness, particularly affecting WMA2, which showed higher rut depths and increased moisture susceptibility.

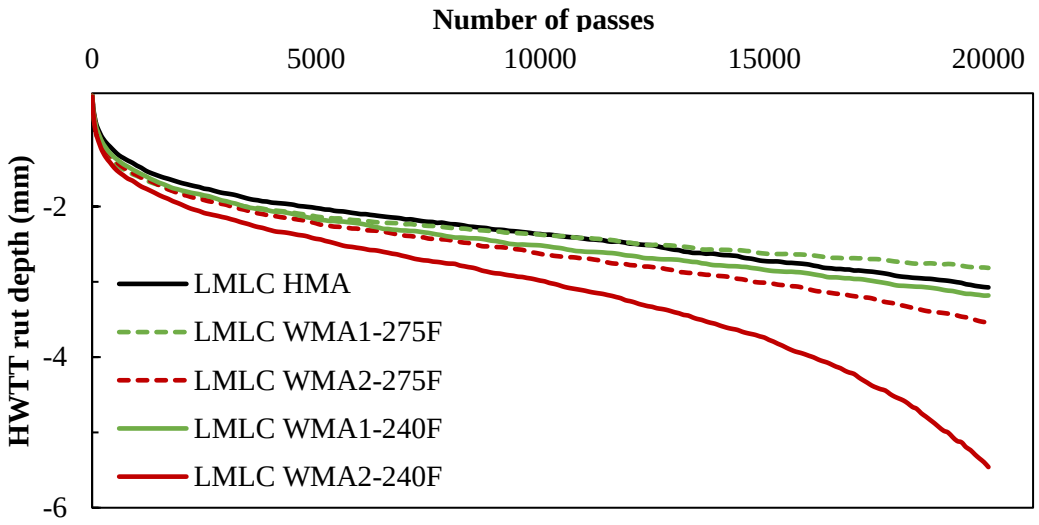

Figure 23. Average HWTT rut depth for LMLC mixtures in Experiment 1

Figure 24 summarizes the final rut depths after 20,000 passes for Experiment 1 mixtures. While WMA mixtures had slightly higher rut depths, especially at the lower STA temperature, all results remained well below the ALDOT-specified limit of 10 mm for PG 76-22 binders (ALDOT, 2022c). The maximum and average coefficients of variation for rut depth were 36.3% and 14.4%, respectively, indicating repeatable test results across replicates.

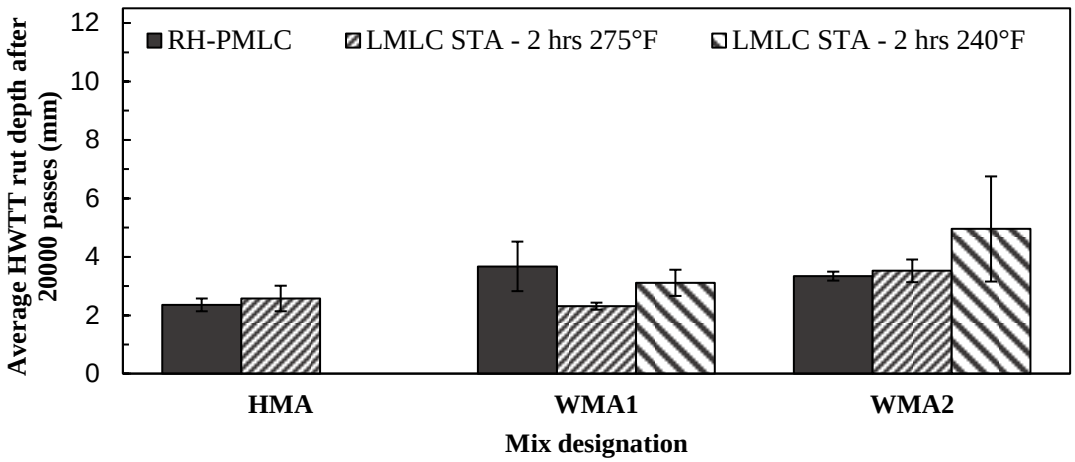

Figure 24. HWTT final rut depth after 20000 passes for the mixtures in Experiment 1

Figure 25 and Figure 26 present HWTT results for Experiment 2 mixtures. The maximum and average COV for rut depths were 33.4% and 23.4%, respectively. Compared to Experiment 1, these mixtures exhibited higher rut depths and showed evidence of the stripping phase, particularly in WMA mixtures. Reduced rutting resistance and increased moisture susceptibility were observed, which can be due to incomplete aggregate drying at lower production temperatures—a known challenge with WMA technologies (Hasan et al., 2015; Hurley & Prowell, 2005). Nevertheless, all mixtures met the HWTT threshold of 10 mm rut depth at 10,000 passes for PG 67-22 virgin binders, indicating acceptable rutting resistance.

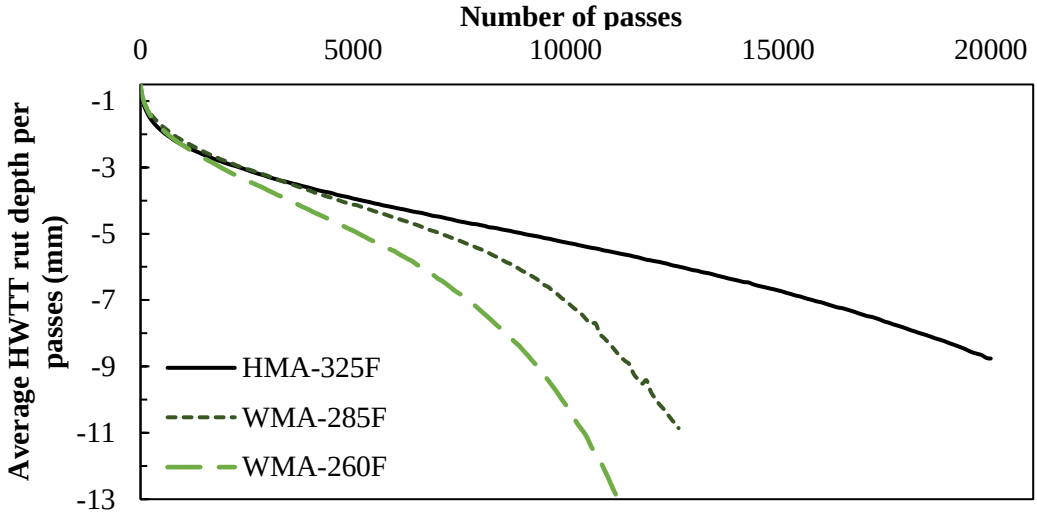

Figure 25. Average HWTT rut depth for H-PMLC samples in Experiment 2

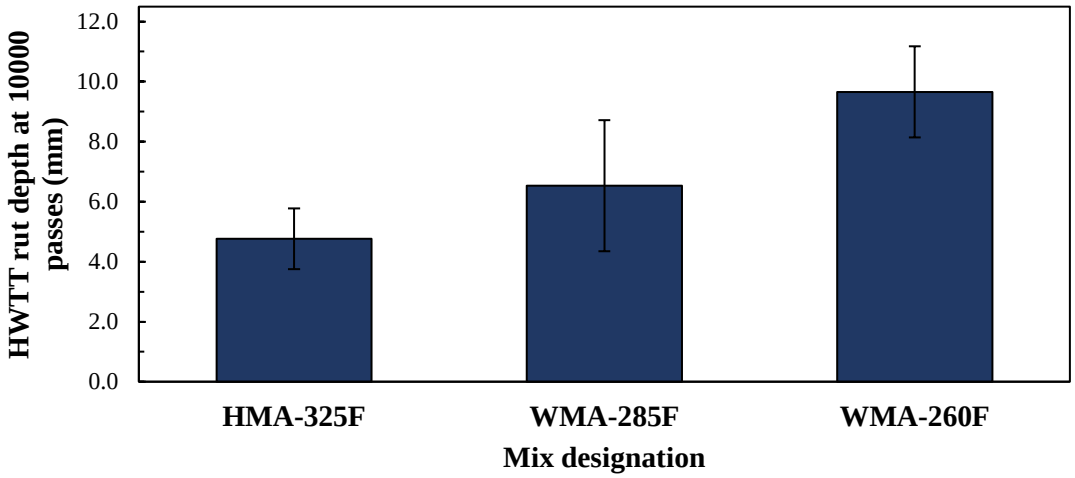

Figure 26. HWTT final rut depth after 10000 passes for H-PMLC samples in Experiment 2

5.3.3 HT-IDT Results

Figure 27 illustrates the average high-temperature indirect tensile strength (HT-ITS) at 50°C for Experiment 1 mixtures, based on four replicate specimens per mixture. The maximum and average coefficients of variation (COV) were 5.3% and 3.3%, respectively, indicating good test repeatability. For RH-PMLC specimens, WMA1 demonstrated HT-ITS comparable to the control HMA, while WMA2 exhibited reduced HT-ITS. For LMLC specimens, WMA mixtures aged at 275°F showed similar strength to the control HMA; however, both WMA mixtures displayed significant reductions in strength at the lower STA temperature of 240°F, aligning with the trends observed in HWTT results. Importantly, all mixtures exceeded the ALDOT-specified threshold of 20 psi (NAPA, 2024), indicating adequate rutting resistance.

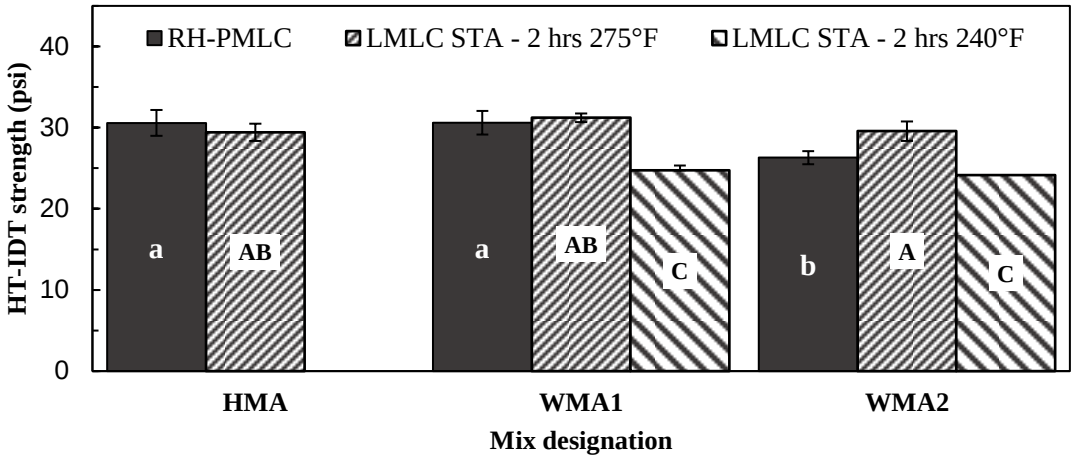

Figure 27. HT-IDT strength for the mixtures in Experiment 1

Figure 28 presents the average HT-ITS values at 50°C for Experiment 2, based on four replicates per mixture. The maximum and average COV were 8.9% and 7.6%, respectively. Both WMA

mixtures exhibited significantly lower HT-ITS values compared to the control HMA mixture, indicating a higher susceptibility to rutting. These results are consistent with the HWTT findings for Experiment 2, further highlighting the impact of reduced production temperatures on the rutting resistance of plant-produced mixtures.

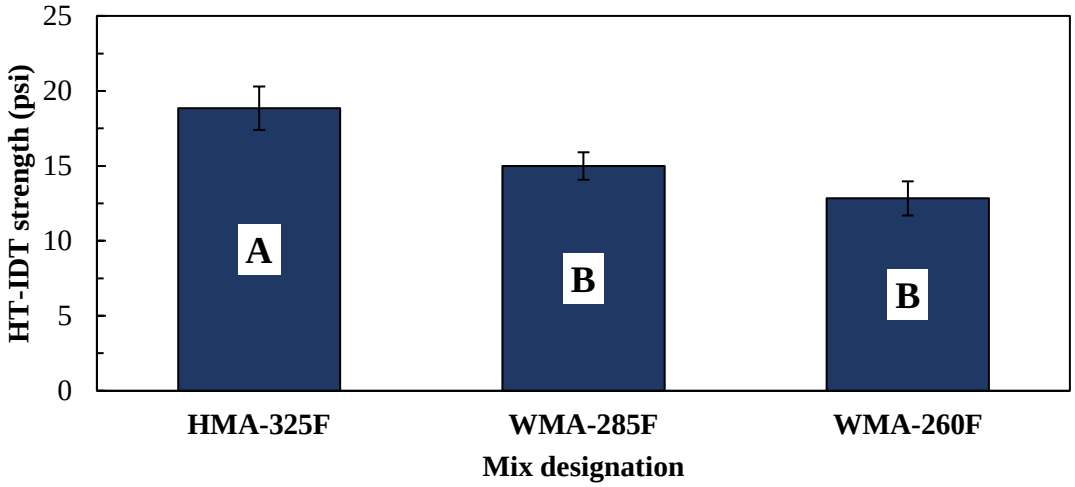

Figure 28. HT-IDT strength for H-PMLC samples in Experiment 2

5.4 Mixture Performance Testing Using AMPT

This section presents the mechanistic performance characteristics of the evaluated asphalt mixtures, measured through AMPT testing. The AMPT tests include dynamic modulus, cyclic fatigue, and stress sweep rutting (SSR) tests. The data collected from these tests provide insight into mixture stiffness, viscoelastic response, cracking resistance and deformation potential, with performance indicators determined using FlexMAT™ and FlexPAVE™ analysis tools.

5.4.1. Dynamic Modulus (|E|) and Phase Angle (δ) Results*

5.4.1.1 |E| Master Curves and δ Black Space Diagrams*

The dynamic modulus (|E*|) master curves and phase angle (δ) black space diagrams for the evaluated mixtures are presented in Figure 29 and Figure 30, respectively. These curves are essential for characterizing each mixture's stiffness and viscoelastic properties across a wide range of loading frequencies and pavement temperatures, reflecting field conditions that pavements will experience over their design life.

As presented in Figure 29a for Experiment 1, both WMA mixtures exhibited lower |E*| values across all temperatures and frequencies compared to the control HMA, with the WMA2 mixture showing the most significant reduction. This reduction in stiffness is often associated with enhanced flexibility and improved cracking resistance, particularly at high and intermediate frequencies, which simulate cold climates and high loading speeds. However, lower |E*| values at low frequencies — which represent higher temperatures or slow-moving traffic — indicate a potential increase in rutting susceptibility due to reduced material stiffness at slow loading.

A similar pattern was observed in Experiment 2, as illustrated in Figure 29b, where the WMA mixtures demonstrated lower dynamic modulus values compared to the control HMA. The WMA mixture produced at 260°F exhibited the lowest stiffness among all evaluated mixtures, further underscoring the impact of reduced production temperatures on mixture stiffness and the need for careful optimization to maintain a balance in performance.

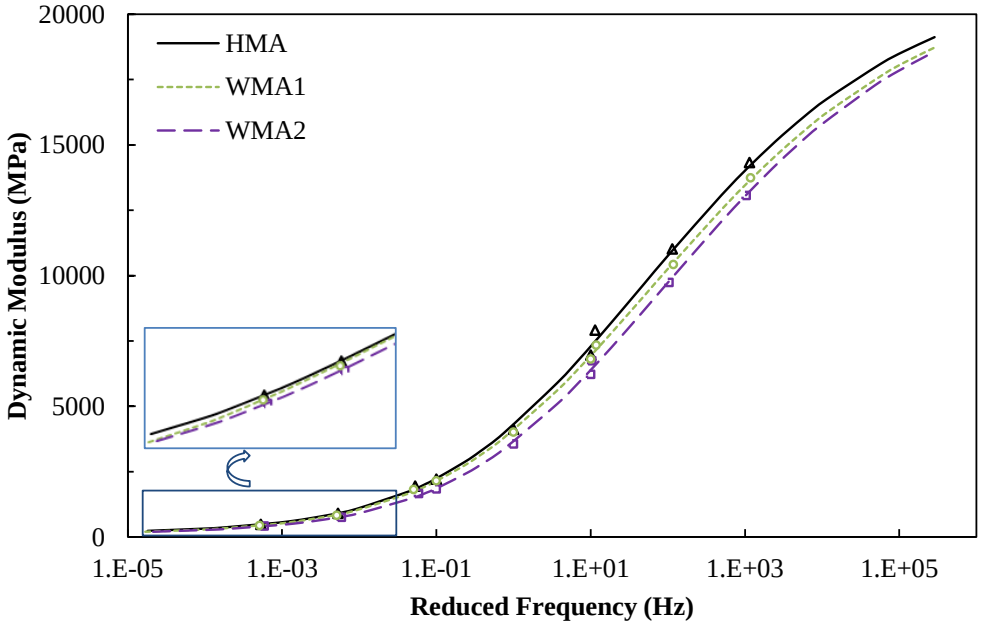

a) Experiment 1 mixtures

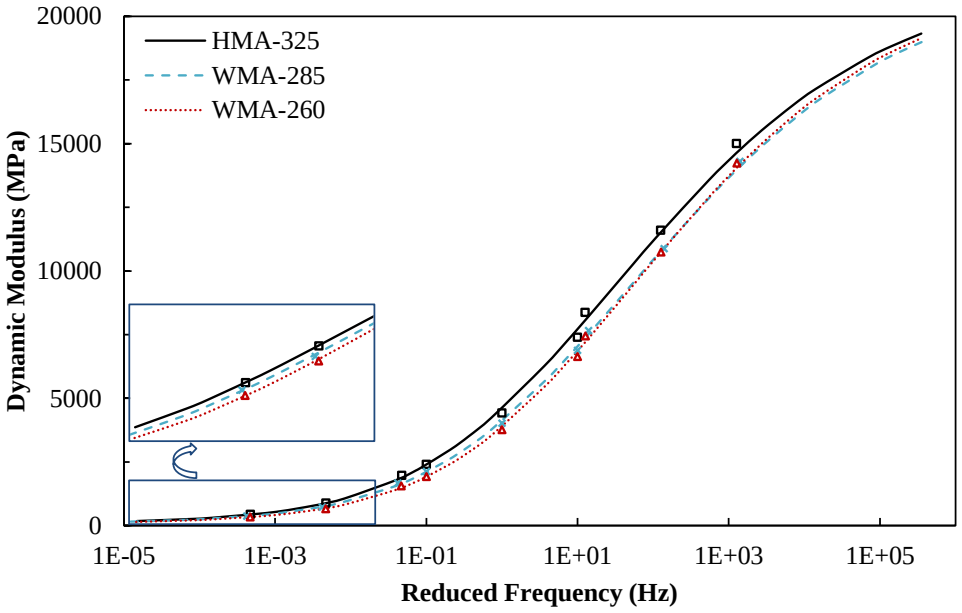

b) Experiment 2 mixtures

Figure 29. Dynamic modulus master curves

The phase angle (δ) black space diagrams, presented in Figure 30, complement the |E*| findings by providing additional insight into the viscoelastic behavior of the mixtures. In Experiment 1 (Figure 30a), the WMA mixtures exhibited higher δ values across most frequencies compared to the control HMA, except at the lowest reduced frequency. Since δ represents the lag between load application and material response, higher δ values reflect more viscous behavior, which typically correlates with improved energy dissipation and better resistance to intermediate- and low-temperature cracking. In contrast, lower δ values at the lowest frequency range correspond to more elastic behavior, which can help mitigate rutting at elevated temperatures.

Experiment 2 results, shown in Figure 30b, showed similar trends, with WMA mixtures showing higher δ values at intermediate and high frequencies and lower δ values at the lowest frequencies. This consistency across both experiments reinforces that WMA technologies and reduced production temperatures shift mixture behavior toward greater flexibility and improved crack resistance. However, these shifts also signal potential trade-offs in rutting performance that must be carefully managed through targeted binder selection, aggregate gradation, and optimized mix design.

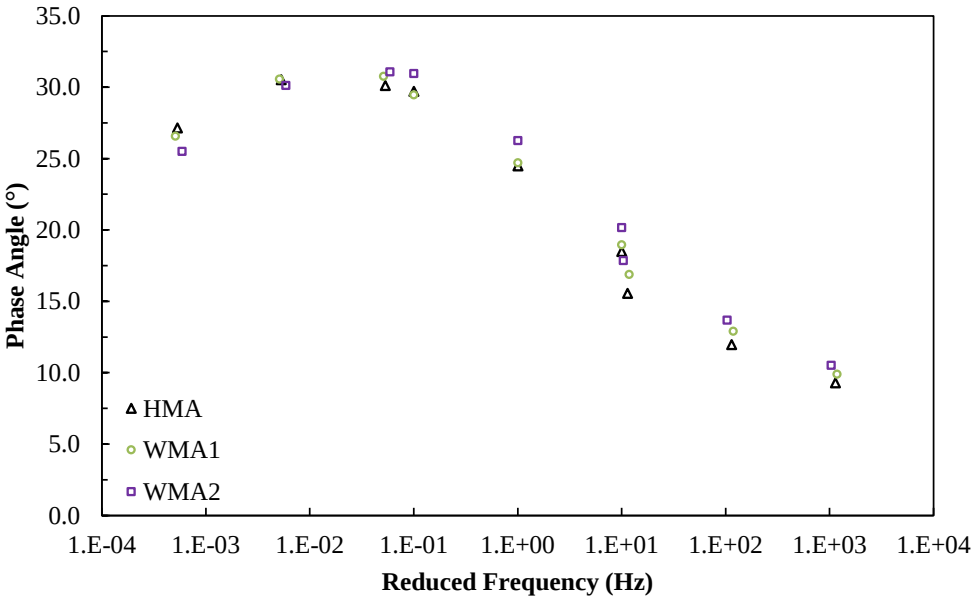

a) Experiment 1 mixtures

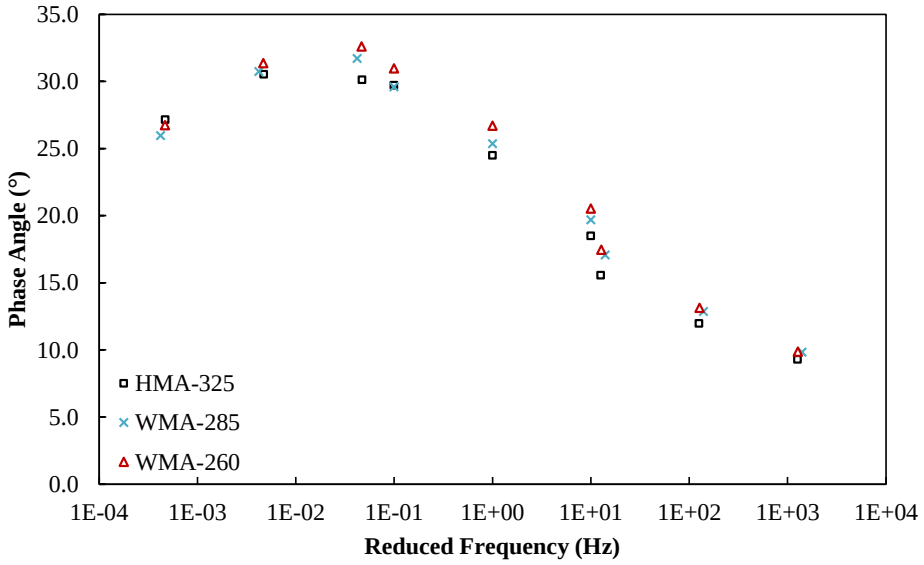

b) Experiment 2 mixtures

Figure 30. Phase angle results

5.4.1.2 Glower Rowe Parameter

The mixture Glover-Rowe parameter (G-R_m) was calculated from |E*| and δ results to capture both mixture stiffness and brittleness, serving as an indicator of cracking resistance. According to NCHRP Project 09-58, the recommended maximum G-R_m values are 8,000 MPa for short-term aged mixtures and 19,000 MPa for long-term aged mixtures (Epps Martin et al., 2020).

Figure 31 illustrates the G-R_m values obtained for RH-PMLC samples. As shown in Figure 31a, both WMA mixtures in Experiment 1 exhibited lower G-R_m values than the control HMA, with WMA2 showing the greatest reduction, suggesting improved cracking resistance. Similarly, as shown in Figure 31b, WMA mixtures in Experiment 2, particularly the WMA produced at 260°F, showed lower G-R_m values, indicating the positive effect of reduced production temperatures on mixture crack resistance.

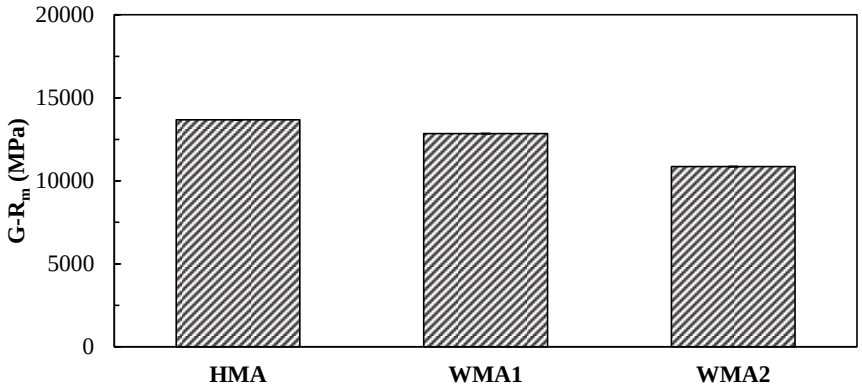

a) Experiment 1 mixtures

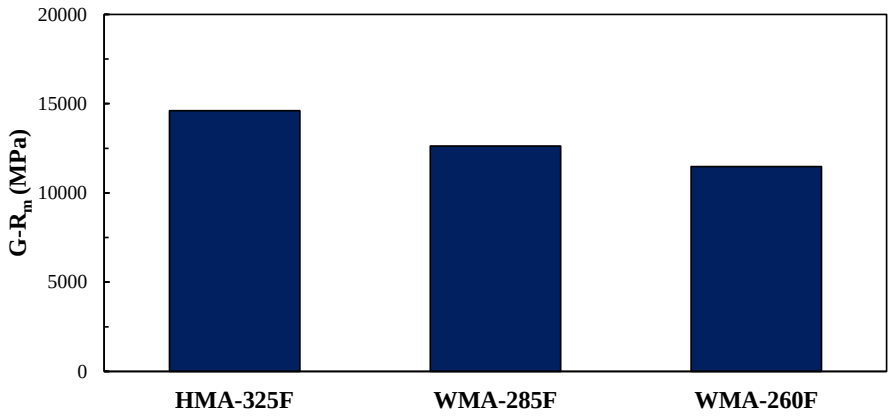

b) Experiment 2 mixtures

Figure 31. G-R_m cracking susceptibility index results

Black space diagrams, plotting |E*| against δ on a log scale, further illustrate these trends in Figure 32. A shift toward the lower right corner represents lower G-R_m values and improved cracking performance. In both experiments, WMA mixtures shifted in this direction, with WMA2 in Experiment 1 and the WMA produced at 260°F in Experiment 2 showing the most improvements. In summary, the G-R_m results and black space diagrams suggest that WMA mixtures produced at lower temperatures can improve cracking resistance by minimizing binder aging relative to conventional HMA.

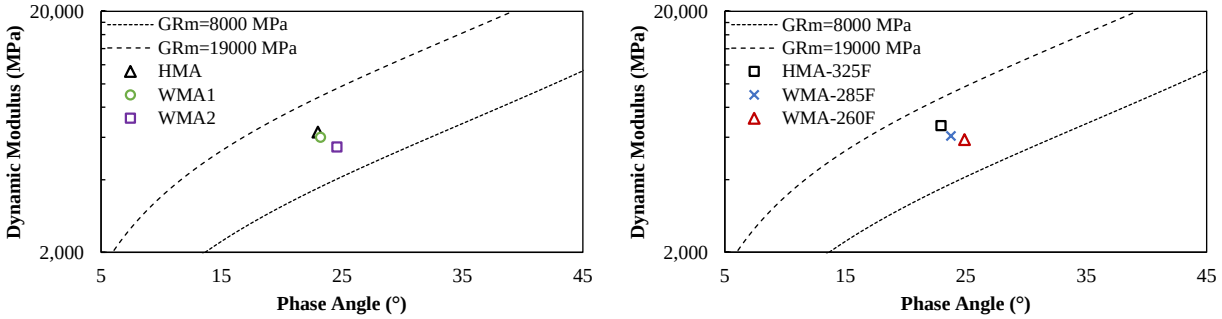

a) Experiment 1 mixtures **b) Experiment 2 mixtures**

Figure 32. Mixture Black Space Diagrams

5.4.2 Cyclic Fatigue Test Results

The cyclic fatigue test results were analyzed using FlexMAT™ v2.2 to evaluate the fatigue damage resistance of the mixtures through the damage characteristics (C-S) curve, as presented in Figure 33. In a C-S curve, pseudo stiffness (C) presents material integrity, which decreases as damage (S) accumulates. A higher and shorter curve indicates faster stiffness loss and more rapid fatigue damage progression (Kim et al., 2021).

Both experiments showed that WMA mixtures exhibited lower but shorter C-S curves compared to the control HMA. This suggests that WMA mixtures are more flexible and capable of absorbing strain energy during early loading but tend to accumulate damage more quickly once fatigue

initiates. The rapid decline in pseudo stiffness suggests that while these mixtures delay initial cracking, they may experience a faster progression of damage under repeated loading. This trade-off highlights the importance of using fatigue parameters and predictive modeling to assess fatigue performance more comprehensively rather than relying solely on C-S curve shape.

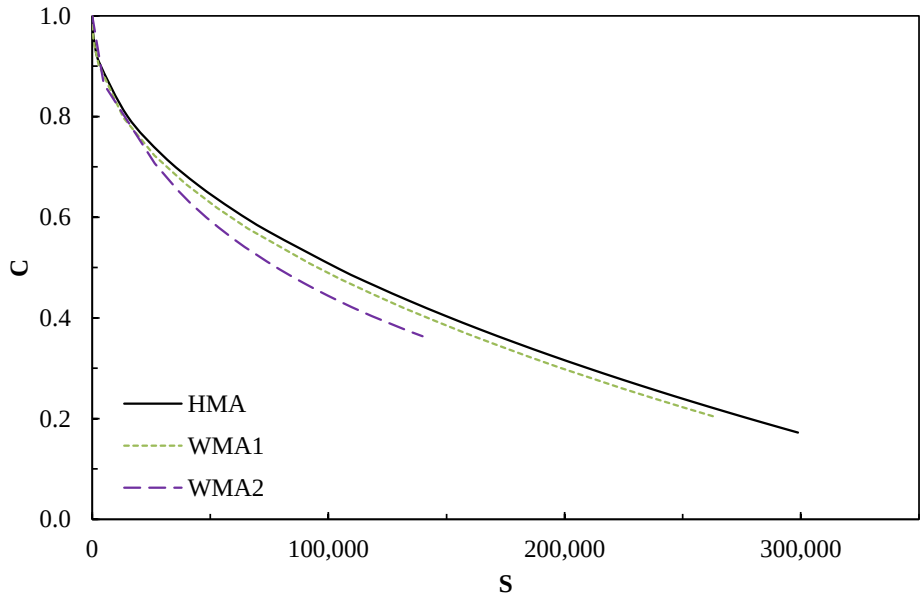

a) Experiment 1 mixtures

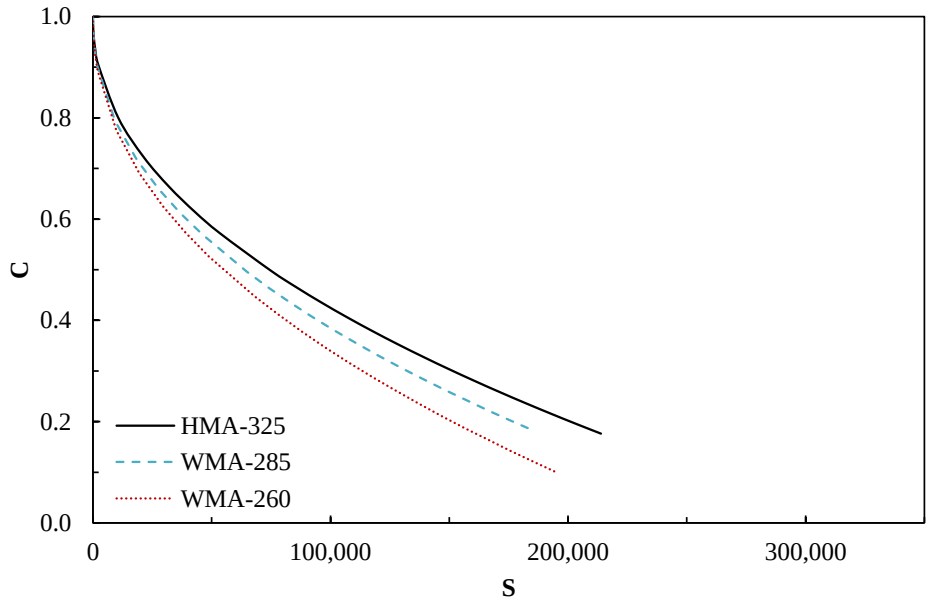

b) Experiment 2 mixtures

Figure 33. Damage Characteristics (C-S curve) results

FlexMAT^{TM} also provides two key fatigue parameters — the D^R failure criterion and the apparent damage capacity (S_{app}) — which offer a more quantitative measure of fatigue resistance. Figure

34 and Figure 35 present these results**.** Mixtures with higher D^R and S_{app} values are expected to perform better in resisting fatigue cracking.

Both experiments showed that the D^R and S_{app} values were comparable among all mixtures, indicating that despite the lower |E*| and the faster damage accumulation observed in C-S curves, the overall fatigue resistance of WMA mixtures remains on par with that of the control HMA. Notably, in Experiment 2, the similarity of D^R and S_{app} values among WMA and HMA mixtures confirms that reducing production temperatures did not negatively impact fatigue performance. This finding is significant, as it suggests that WMA technologies can be adopted without compromising structural durability, even when produced at lower temperatures.

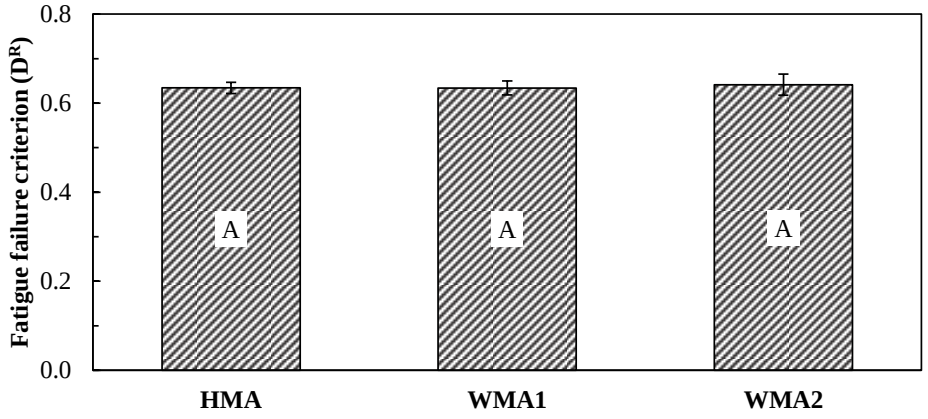

a) Experiment 1 mixtures

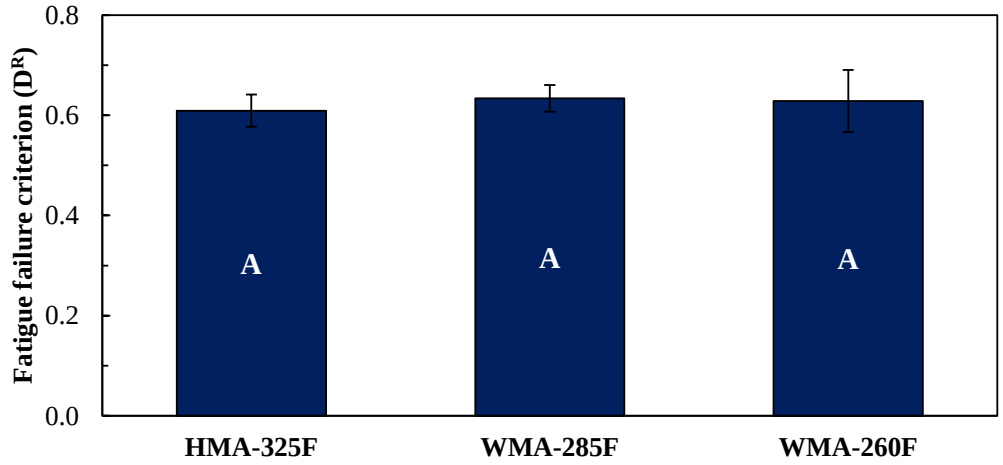

b) Experiment 2 mixtures

Figure 34. Fatigue failure criterion (D^R) results

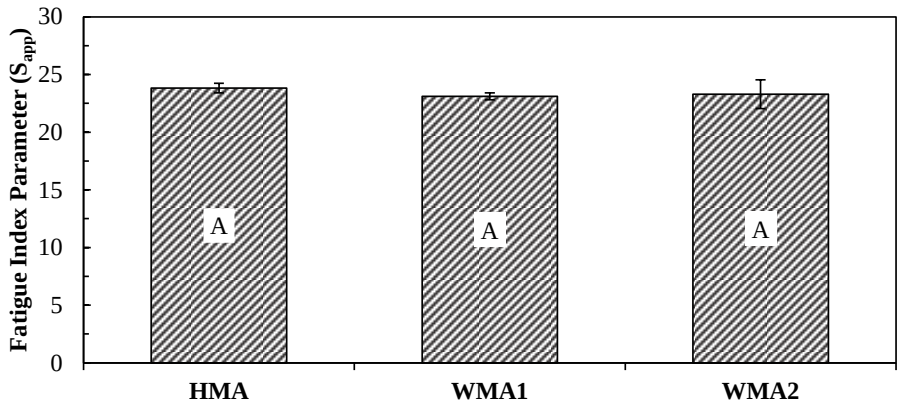

a) Experiment 1 mixtures

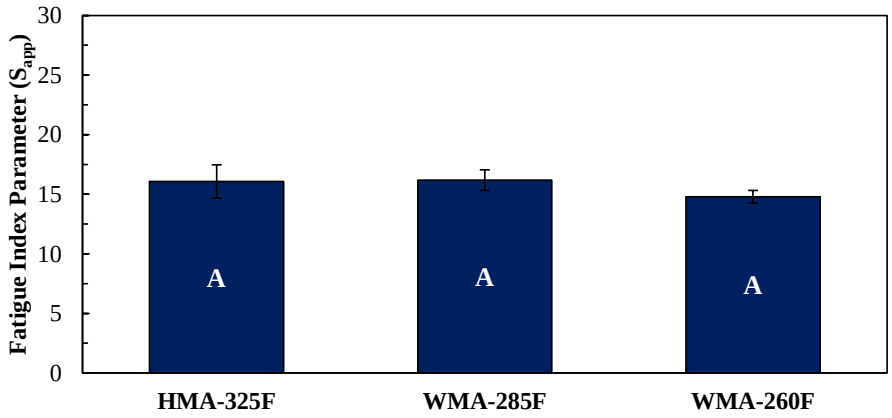

b) Experiment 2 mixtures

Figure 35. Fatigue index parameter (S_{app}) results

5.4.3. Stress Sweep Rutting Results

Figure 36 and Figure 37 illustrate permanent strain results captured during high- and low-temperature SSR tests. In both experiments, WMA mixtures exhibited higher permanent strain values than the control HMA at both temperature conditions. This behavior is attributed to lower mixture stiffness, resulting from reduced production temperatures and lower binder aging levels. The softest mixtures — WMA2 in Experiment 1 and the WMA produced at 260°F in Experiment 2 — showed the highest permanent strains, consistent with trends observed in |E*| and BMD performance tests. These results indicate that while WMA mixtures gain flexibility and crack resistance, they may deform more under heavy loads.

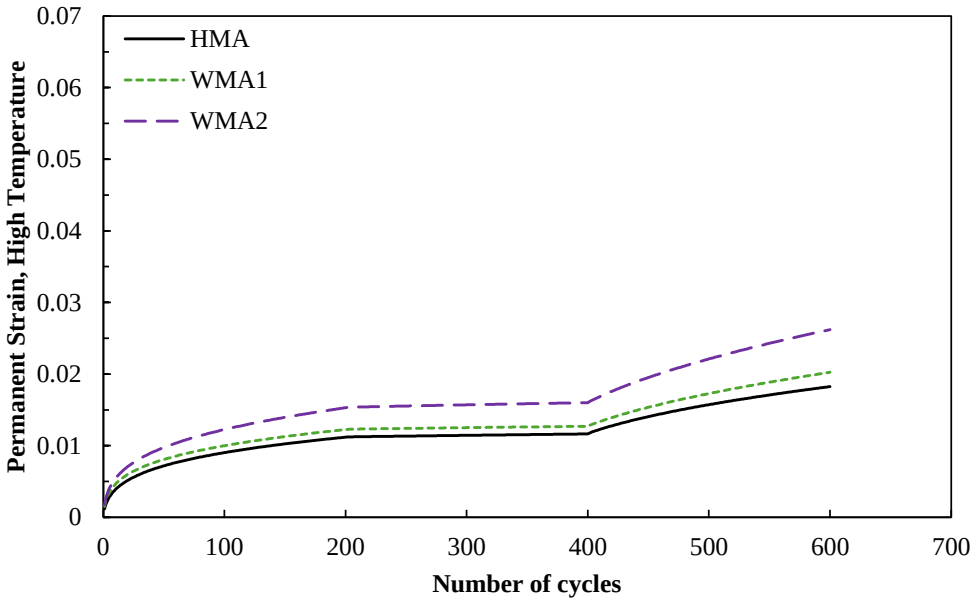

a) Experiment 1 mixtures

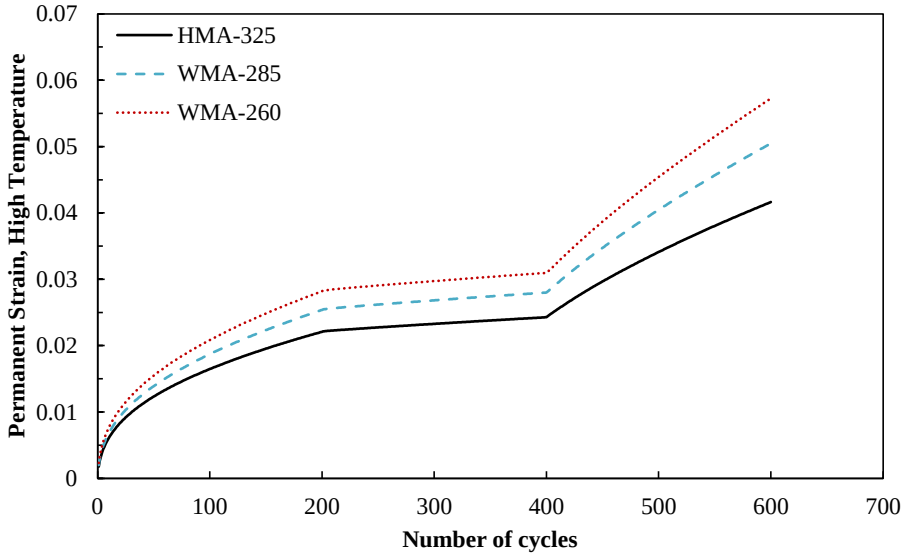

b) Experiment 2 mixtures

Figure 36. Permanent strain captures during high-temperature SSR test

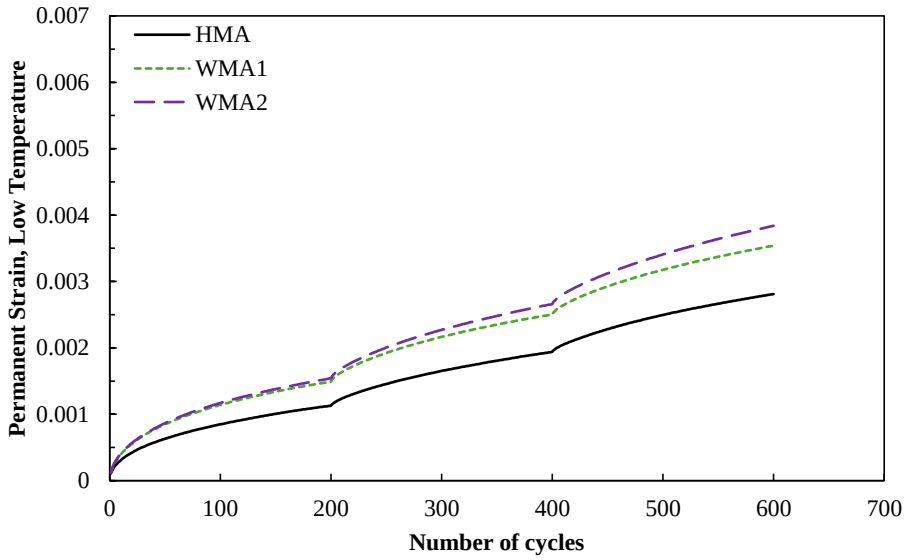

a) Experiment 1 mixtures

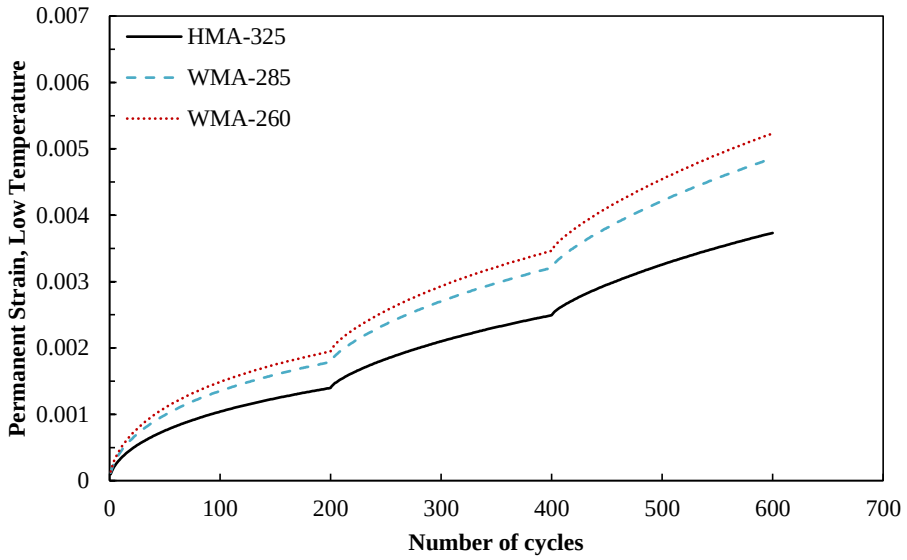

b) Experiment 2 mixtures

Figure 37. Permanent strain captures during low-temperature SSR test

The long-term rutting susceptibility of the mixtures was evaluated using the rutting susceptibility index (RSI), shown in Figure 38. RSI estimates the mean percentage of permanent strain in an asphalt layer over a 20-year period under 30 million ESALs. Lower RSI values are desirable, indicating better rutting resistance. In both experiments, WMA mixtures exhibited higher RSI values than the control HMA. In Experiment 1, WMA2 had the highest RSI, highlighting the influence of the WMA additive on rutting behavior. In Experiment 2, RSI values increased as production temperatures decreased, with the WMA produced at 260°F showing the highest rutting susceptibility. This trend confirms that reduced aging at lower production temperatures can lead to softer mixtures that are less rutting resistance.

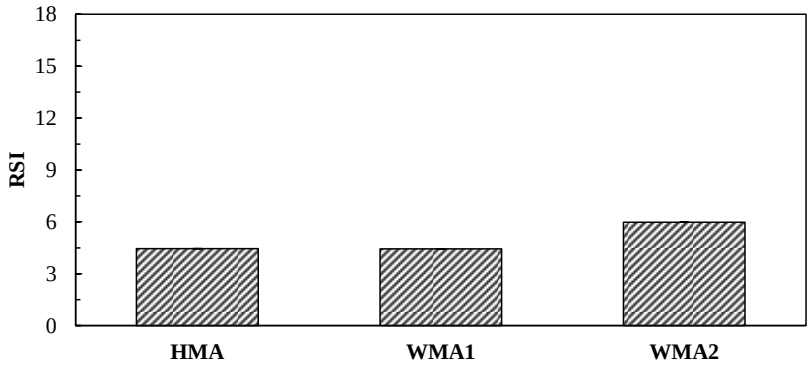

a) Experiment 1 mixtures

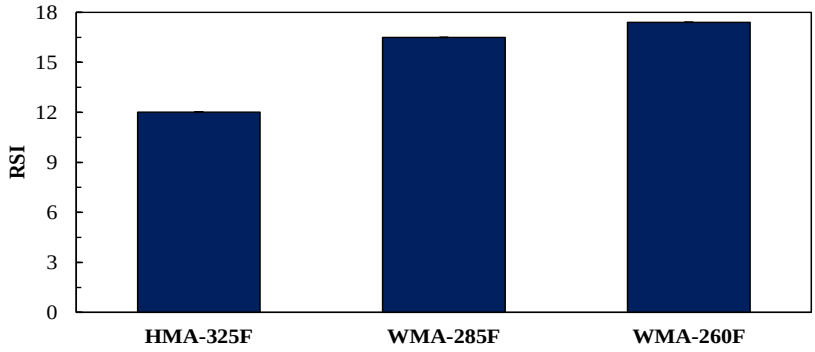

b) Experiment 2 mixtures

Figure 38. RSI rutting index results

5.5 Predicted Performance Using FlexPAVE™ Modeling

This section presents a comparative analysis of the predicted long-term performance of pavement structures using the FlexPAVE™ pavement analysis tool. The analysis incorporates project-specific climate and traffic data, pavement cross-section configurations, and asphalt mixture properties derived from AMPT testing to evaluate fatigue and rutting performance throughout the pavement service life.

Figure 39 shows the predicted percent fatigue damage over 20 years for Experiments 1 and 2. In both experiments, WMA mixtures exhibited slightly higher predicted damage compared to the control HMA. This increase is consistent with the softer characteristics and faster damage progression observed in the laboratory C-S curves. However, except for WMA2, the predicted increase in percent damage after 20 years ranged from only 0.3% to 2.6%, indicating that the field fatigue performance of WMA mixtures is expected to remain comparable to that of conventional HMAs. The small differences confirm that while reduced production temperatures may accelerate binder softening and aging effects, these changes remain manageable within typical pavement structures and are not likely to compromise long-term performance.

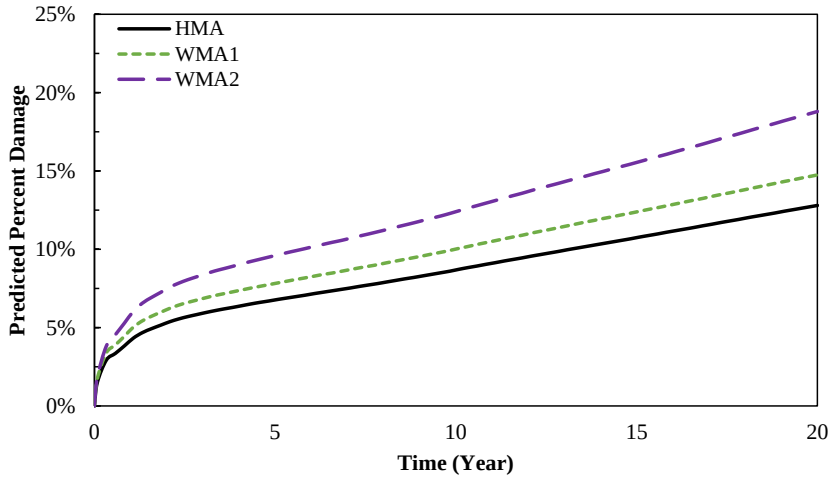

a) Experiment 1 mixtures

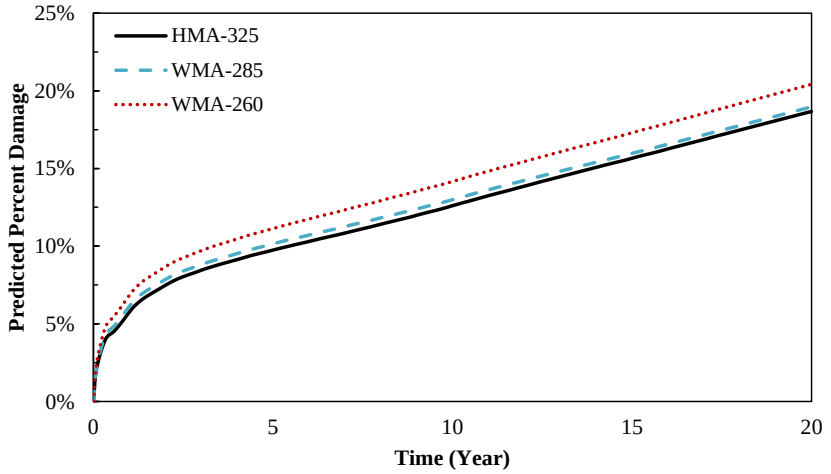

b) Experiment 2 mixtures

Figure 39. Predicted percent damage using FHWA's FlexPave™ modeling

Predicted rutting performance, shown in Figure 40, offers further insight. In Experiment 1, WMA1 showed rutting performance similar to the control HMA, while WMA2 showed higher rut accumulation, reflecting its greater susceptibility observed in SSR tests and higher permanent strain values. In Experiment 2, both WMA mixtures exhibited greater rut accumulation than the control HMA, with rutting increasing as production temperatures decreased. This trend confirms that reduced aging and binder stiffening at lower production temperatures result in softer mixtures that are less resistant to deformation under repeated loading.

Despite these increases, predicted rut depths for all mixtures remained within acceptable performance thresholds, not exceeding 0.4 inches (10 mm) after 20 years. Additionally, the rate of rut depth growth was notably lower in Experiment 1 than in Experiment 2. This suggests that the polymer-modified binder (PG 76-22) used in Experiment 1 contributed to improved rutting resistance, compensating for less aging due to lower production temperatures. The ability of WMA1 to match the rutting performance of the control HMA demonstrates that the impacts of

WMA production on rutting susceptibility can be effectively mitigated through binder selection and mix design optimization.

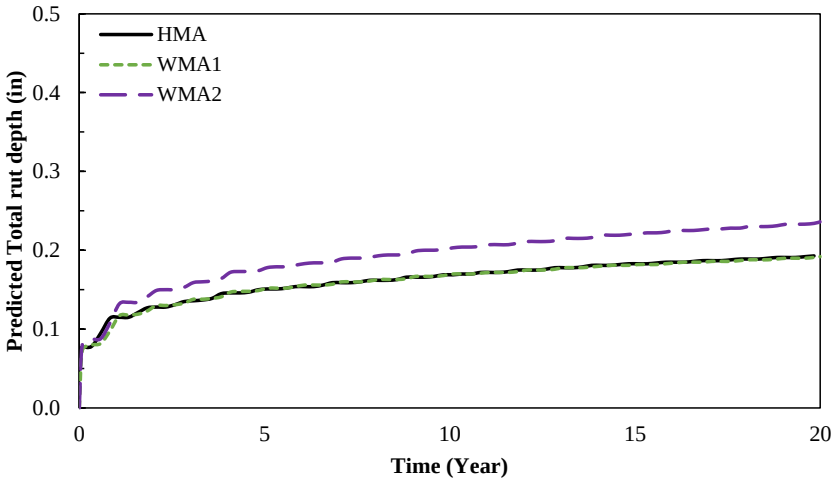

a) Experiment 1 mixtures

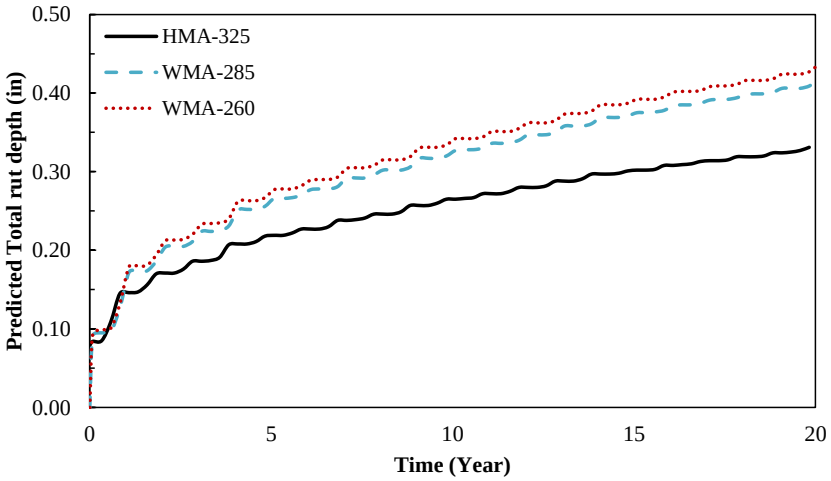

b) Experiment 2 mixtures

Figure 40. Predicted total rut depth using FHWA's FlexPave™ modeling

Overall, the predicted results from FlexPAVE™ modeling confirm that WMA mixtures can achieve long-term field performance comparable to conventional HMAs. The changes in fatigue and rutting damage were mix-specific and remained within acceptable limits, which could be addressed by appropriate mixture design adjustments.

6. CONCLUSIONS

This study evaluated the effects of reducing asphalt mixture production temperatures using WMA Technologies, focusing on energy savings and key mixture performance characteristics. Two controlled experiments were conducted using ALDOT-approved HMA mix designs. The first experiment compared two WMA mixtures produced with chemical additives to a conventional

HMA mixture. The second experiment further reduced production temperatures to explore additional energy savings and assess their impact on mixture performance.

- **Energy Consumption Reduction**: Lowering production temperatures using WMA technologies resulted in measurable reductions in burner fuel consumption. Specifically, reducing production temperatures by 40°F (22°C) and 65°F (36°C) led to burner fuel savings of 8% and 19%, respectively, compared to the control HMA. These findings demonstrate that meaningful energy savings can be achieved without requiring significant changes to existing production.
- **Binder Rheological Properties**: Extracted binders from the WMA mixtures exhibited slightly lower high-temperature continuous grades relative to the HMA binder, though no differences were observed in the PG grades. Higher J_{nr} values from MSCR testing may indicate a slightly decreased resistance to rutting in the WMA binders, likely due to reduced oxidative aging at lower production temperatures. Additionally, similar low-temperature continuous grades were observed for extracted binders from WMA and HMA mixtures.
- **Cracking Resistance (BMD Testing)**: Cracking resistance, evaluated using the CT_{Index} test, was found to be similar for both plant-mixed WMA and HMA specimens. However, in Experiment 1, the LMLC specimens for WMA mixtures showed significantly higher CT_{Index} values, indicating better cracking resistance. This difference may be attributed to differences in short-term aging between laboratory conditions and those at the plant. This finding suggests that further research in this area is necessary.
- **Rutting Resistance and Moisture Susceptibility (BMD Testing)**: The rutting and moisture resistance of WMA mixtures were generally lower than those of the HMA control, although they still met the ALDOT rutting thresholds. These results highlight the importance of verifying rutting resistance and moisture susceptibility when production temperatures are reduced, as changes in mixture stiffness and binder properties can influence field performance. Adjustments to the mix design may be needed to offset these changes.
- **Cracking Performance (AMPT Testing)**: AMPT-based testing confirmed that WMA mixtures produced at lower temperatures exhibited improved low-temperature cracking resistance, as reflected in the dynamic modulus master curves and Glover-Rowe ($G\text{-}R_m$) parameters. Fatigue parameters (D^R and S_{app}) were comparable between WMA and HMA mixtures, indicating that reduced production temperatures did not negatively affect fatigue performance.
- **Rutting Performance (AMPT Testing)**: SSR test results showed that WMA mixtures were less resistant to rutting than the control HMA mixtures, particularly at the lowest production temperatures. This finding is consistent with binder and mixture stiffness results, emphasizing the need for verifying rutting resistance when targeting aggressive temperature reductions.
- **Predicted Performance (FlexPave™ modeling):** FlexPAVE™ modeling showed slightly higher cumulative fatigue damage and rutting for WMA mixtures relative to the HMA control. However, the increases in fatigue damage were generally modest, and predicted rut depths remained within acceptable limits.

The results of this study support the use of WMA technologies to lower production temperatures, leading to measurable energy savings while preserving pavement performance. Laboratory tests and predictive modeling indicate that the cracking resistance of WMA mixtures is comparable to that of HMA mixtures. However, the study shows a reduction in rutting and moisture resistance, which underscores the need for careful consideration when implementing WMA technologies within the BMD framework. Adjustments may be necessary to meet BMD requirements. This study provides valuable insights for agencies and contractors looking to integrate WMA technologies into their paving operations, allowing them to benefit from reduced production temperatures while still meeting the performance standards required for asphalt mixtures.

REFERENCES

AASHTO. (2021). AASHTO R84-17 (2021): Standard Practice for Developing Dynamic Modulus Master Curves for Asphalt Mixtures Using the Asphalt Mixture Performance Tester (AMPT). In. ASTM Compass.

AASHTO. (2022a). AASHTO M323-22 Standard Specification for Superpave Volumetric Mix Design. In.

AASHTO. (2022b). AASHTO T313-22 Standard Method of Test for Determining the Flexural Creep Stiffness of Asphalt Binder Using the Bending Beam Rheometer (BBR). In.

AASHTO. (2022c). AASHTO TP134-22 Standard Method of Test for Stress Sweep Rutting (SSR) Test Using Asphalt Mixture Performance Tester (AMPT). In.

AASHTO. (2023a). AASHTO 29-15 (2023) Standard Practice for Grading or Verifying the Performance Grade (PG) of an Asphalt Binder. In.

AASHTO. (2023b). AASHTO R30-22 Standard Practice for Laboratory Conditioning of Asphalt Mixtures. In.

AASHTO. (2023c). AASHTO T132-23 Standard Method of Test for Determining the Dynamic Modulus for Asphalt Mixtures Using Small Specimens in the Asphalt Mixture Performance Tester (AMPT). In.

AASHTO. (2023d). AASHTO T324-23 Standard Method of Test for Hamburg Wheel-Track Testing of Compacted Asphalt Mixtures. In.

AASHTO. (2023e). AASHTO T350-19 (2023) Standard Method of Test for Quantitative Extraction of Asphalt Binder from Asphalt Mixtures. In.

AASHTO. (2024a). AASHTO T164-24 Standard Method of Test for Quantitative Extraction of Asphalt Binder from Asphalt Mixtures. In.

AASHTO. (2024b). AASHTO T315-24 Standard Method of Test for Determining the Rheological Properties of Asphalt Binder Using a Dynamic Shear Rheometer (DSR). In.

AASHTO. (2024c). AASHTO T411-24 Standard Method of Test for Determining the Damage Characteristic Curve and Failure Criterion Using Small Specimens in the Asphalt Mixture Performance Tester (AMPT) Cyclic Fatigue Test. In.

Akentuna, M., Mohammad, L. N., Boateng, K. A., & Cooper Jr, S. (2022). Warm Mix Asphalt demonstration projects in Louisiana: Case study of five to eight years of field performance. *Transportation research record*, *2676*(9), 148-158.

ALDOT. (2022a). ALDOT-458 High Temperature Indirect Tensile Test for HMA. In.

ALDOT. (2022b). Standard Specifications for Highway Construction, Section 424 (d). In. https://www.dot.state.al.us/publications/Construction/Specifications.html.

ALDOT. (2022c). Standard Specifications for Highway Construction, Section 424.02 (c). In. https://www.dot.state.al.us/publications/Construction/Specifications.html.

ALDOT. (2022d). Standard Specifications for Highway Construction, Section 424.02 (e). In. https://www.dot.state.al.us/publications/Construction/Specifications.html.

ASTM. (2019). ASTM D8225 - 19 Standard Practice for Determination of Cracking Tolerance Index of Asphalt Mixture Using the Indirect Tensile Cracking Test at Intermediate Temperature. In.

ASTM. (2022). ASTM D7643 - 22 Standard Practice for Determining the Continuous Grading Temperatures and Continuous Grades for PG Graded Asphalt Binders. In.

ASTM. (2024). ASTM D5404/D5404M − 24 Standard Practice for Recovery of Asphalt Binder from Solution Using the Rotary Evaporator. In.

Bairgi, B. K., Manna, U. A., & Tarefder, R. A. (2019). Tribological evaluation of asphalt binder with chemical warm-mix additives. International Airfield and Highway Pavements Conference 2019,

Capitão, S., Picado-Santos, L., & Martinho, F. (2012). Pavement engineering materials: Review on the use of warm-mix asphalt. *Construction and Building Materials*, *36*, 1016-1024.

Caputo, P., Abe, A. A., Loise, V., Porto, M., Calandra, P., Angelico, R., & Oliviero Rossi, C. (2020). The role of additives in warm mix asphalt technology: An insight into their mechanisms of improving an emerging technology. *Nanomaterials*, *10*(6), 1202.

Cheraghian, G., Falchetto, A. C., You, Z., Chen, S., Kim, Y. S., Westerhoff, J., Moon, K. H., & Wistuba, M. P. (2020). Warm mix asphalt technology: An up to date review. *Journal of cleaner production*, *268*, 122128.

Croteau, J.-M., & Tessier, B. (2008). Warm mix asphalt paving technologies: a road builder's perspective. Annual Conference of the Transportation Association of Canada, Toronto,

Dao, D. V., Nguyen, N.-L., Nguyen, M. H., Ly, H.-B., & Truong, V. Q. (2022). Evaluation of cracking resistance of warm mix asphalt incorporating high reclaimed asphalt pavement content. *Proceedings of the Institution of Mechanical Engineers, Part L: Journal of Materials: Design and Applications*, *236*(12), 2550-2560.

Environmental Protection Agency. (2024). *Managing Used Oil: Answers to Frequent Questions for Businesses*. Retrieved July 31, 2024 from https://www.epa.gov/hw/managing-used-oil-answers-frequent-questions-businesses

Epps, J. A. (2019). Innovative asphalt pavement technology: paving the way for the world's roadways. *Transportation research record*, *2673*(1), 1-16.

Epps Martin, A., Kaseer, F., Arámbula-Mercado, E., Bajaj, A., Cucalon, L. G., Yin, F., Chowdhury, A., Epps, J., Glover, C., & Hajj, E. Y. (2020). *Evaluating the effects of recycling agents on asphalt mixtures with high RAS and RAP binder ratios*.

Eslaminia, M., & Guddati, M. N. (2016). Fourier-finite element analysis of pavements under moving vehicular loading. *International Journal of Pavement Engineering*, *17*(7), 602-614.

Fakhri, M., Arzjani, D., Ayar, P., Mottaghi, M., & Arzjani, N. (2021). Performance Evaluation of WMA Containing Re-Refined Acidic Sludge and Amorphous Poly Alpha Olefin (APAO). *Sustainability*, *13*(6), 3315.

Federal Highway Administration. (2025). *Federal Highway Administration Asphalt Material Analysis Tools* Retrieved January 31, 2025 from https://highways.dot.gov/research/infrastructure/pavements/flexmat

Gandhi, T., Akisetty, C., & Amirkhanian, S. (2009). Laboratory evaluation of warm asphalt binder aging characteristics. *International Journal of Pavement Engineering*, *10*(5), 353-359.

Garcia Cucalon, L., Kassem, E., Little, D. N., & Masad, E. (2017). Fundamental evaluation of moisture damage in warm-mix asphalts. *Road Materials and Pavement Design*, *18*(sup1), 258-283.

Ghanbari, A., Underwood, B. S., & Kim, Y. R. (2022). Development of a rutting index parameter based on the stress sweep rutting test and permanent deformation shift model. *International Journal of Pavement Engineering*, *23*(2), 387-399.

Hasan, M. R. M., You, Z., Porter, D., & Goh, S. W. (2015). Laboratory moisture susceptibility evaluation of WMA under possible field conditions. *Construction and Building Materials*, *101*, 57-64.

Hurley, G. C., & Prowell, B. D. (2005). Evaluation of Aspha-Min zeolite for use in warm mix asphalt. *NCAT report*(05-04).

Hurley, G. C., Prowell, B. D., & Kvasnak, A. N. (2009). Michigan field trial of warm mix asphalt technologies: construction summary. *National Center for Asphalt Technology, Auburn, AL, USA*.

Jamshidi, A., Hamzah, M. O., & You, Z. (2013). Performance of warm mix asphalt containing Sasobit®: State-of-the-art. *Construction and Building Materials*, *38*, 530-553.

Jones, D. (2013). *Warm-Mix Asphalt Study: Field Test Performance Evaluation*. University of California Pavement Research Center Report UCPRC-TM-2013-08.

Kim, Y. R., Castorena, C., Saleh, N. F., Braswell, E., Elwardany, M., & Rad, F. Y. (2021). *Long-term aging of asphalt mixtures for performance testing and prediction: Phase III results*.

Milad, A., Babalghaith, A. M., Al-Sabaeei, A. M., Dulaimi, A., Ali, A., Reddy, S. S., Bilema, M., & Yusoff, N. I. M. (2022). A comparative review of hot and warm mix asphalt technologies from environmental and economic perspectives: towards a sustainable asphalt

pavement. *International Journal of Environmental Research and Public Health*, *19*(22), 14863.

NAPA. (2023). NAPA IS-145 Guide on Asphalt Mixture Specimen Fabrication for BMD Performance Testing. In.

NAPA. (2024). *Balanced Mix Design (BMD) Resource Guide*. Retrieved Jule 31, 2024 from https://www.asphaltpavement.org/expertise/engineering/resources/bmd-resource-guide

Oshone, M., Sias, J. E., Dave, E. V., Epps Martin, A., Kaseer, F., & Rahbar-Rastegar, R. (2019). Exploring master curve parameters to distinguish between mixture variables. *Road Materials and Pavement Design*, *20*(sup2), S812-S826.

Prowell, B. D., Hurley, G. C., & Frank, B. (2012). *Warm-mix asphalt: Best practices*. National Asphalt Pavement Association.

Rubio, M. C., Martínez, G., Baena, L., & Moreno, F. (2012). Warm mix asphalt: an overview. *Journal of cleaner production*, *24*, 76-84.

Sukhija, M., Saboo, N., & Pani, A. (2022). Economic and environmental aspects of warm mix asphalt mixtures: A comparative analysis. *Transportation Research Part D: Transport and Environment*, *109*, 103355.

Wang, Y., Norouzi, A., & Kim, Y. R. (2016). Comparison of fatigue cracking performance of asphalt pavements predicted by pavement ME and LVECD programs. *Transportation research record*, *2590*(1), 44-55.

Wang, Y. D., Ghanbari, A., Underwood, B. S., & Kim, Y. R. (2021). Development of preliminary transfer functions for performance predictions in FlexPAVE™. *Construction and Building Materials*, *266*, 121182.

Wen, H., Wu, S., Mohammad, L. N., Zhang, W., Shen, S., & Faheem, A. (2016). Long-term field rutting and moisture susceptibility performance of warm-mix asphalt pavement. *Transportation research record*, *2575*(1), 103-112.

West, R., Rodezno, C., Julian, G., Prowell, B., Frank, B., Osborn, L. V., & Kriech, T. (2014). *Field performance of warm mix asphalt technologies*.

West, R., Rodezno, C., Julian, G., & Prowell, D. (2014). Engineering properties and field performance of warm mix asphalt technologies. *National Cooperative Highway Research Program, Washington, DC, USA, NCHRP Final Report Project*(09-47A).

Williams, B. A., Willis, J. R., & Shacat, J. (2024). *Asphalt Pavement Industry Survey on Recycled Materials and Warm-Mix Asphalt Usage: 2022*. National Asphalt Pavement Association Information Series 138.

Yin, F., Chen, C., Moraes, R., Hanz, A., Hehir, J., & Knudtson, D. (2023). *Impact of Polymer Modification on IDEAL-CT and I-FIT for Cracking Resistance Evaluation of Asphalt Mixtures*.

Yin, F., West, R., Powell, B., & DuBois, C. (2023). Short-term performance characterization and fatigue damage prediction of asphalt mixtures containing polymer-modified binders and recycled plastics. *Transportation research record*, 03611981221143119.

Zaumanis, M. (2014). Warm mix asphalt. In *Climate change, energy, sustainability and pavements* (pp. 309-334). Springer.

Zhang, R., Sias, J. E., & Dave, E. V. (2022). Evaluation of the cracking and aging susceptibility of asphalt mixtures using viscoelastic properties and master curve parameters. *Journal of Traffic and Transportation Engineering (English Edition)*, *9*(1), 106-119.

Zhou, F., Im, S., Sun, L., & Scullion, T. (2017). Development of an IDEAL cracking test for asphalt mix design and QC/QA. *Road Materials and Pavement Design*, *18*(sup4), 405-427.